An inter-comparison of tropospheric ozone reanalysis products from CAMS, CAMS-Interim, TCR-1 and TCR-2

Vincent Huijnen[1], Kazuyuki Miyazaki[2], Johannes Flemming[3], Antje Inness[3], Takashi Sekiya[4], Martin G. Schultz[5]

[1] Royal Netherlands Meteorological Institute, De Bilt, the Netherlands
[2] Jet Propulsion Laboratory, California Institute of Technology, Pasadena, CA 91109, USA
[3] ECMWF, Shinfield Park, Reading, RG2 9AX, UK
[4] Research Institute for Global Change (RIGC), Japan Agency for Marine–Earth Science and Technology (JAMSTEC), Yokohama 2360001, Japan
[5] Jülich Supercomputing Centre, Forschungszentrum Jülich, Jülich, Germany

Correspondence to: V. Huijnen (Vincent.Huijnen@knmi.nl)

Abstract. Global tropospheric ozone reanalyses constructed using different state-of-the-art satellite data assimilation systems, prepared as part of the Copernicus Atmosphere Monitoring Service (CAMS-iRean and CAMS-Rean) as well as two fully independent Tropospheric Chemistry Reanalyses (TCR-1 and TCR-2), have been inter-compared and evaluated for the past decade. The updated reanalyses (CAMS-Rean and TCR-2) generally show substantially improved agreements with independent ground and ozonesonde observations over their predecessor versions (CAMS-iRean and TCR-1) for the diurnal, synoptical, seasonal, and interannual variability. For instance, for the NH mid latitudes the tropospheric ozone columns (surface to 300 hPa) from the updated reanalyses show mean biases to within 0.8 DU (3% relative to the observed column) with respect to the ozonesonde observations. The improved performance can likely be attributed to a mixture of various upgrades, such as revisions in the chemical data assimilation, including the assimilated measurements, and the forecast model performance. The updated chemical reanalyses agree well with each other for most cases, which highlights the usefulness of the current chemical reanalyses in a variety of studies. Meanwhile, significant temporal changes in the reanalysis quality in all the systems can be attributed to discontinuities in the observing systems. To improve the temporal consistency, a careful assessment of changes in the assimilation configuration, such as a detailed assessment of biases between various retrieval products, is needed. Our comparison suggests that improving the observational constraints, including the continued development of satellite observing systems, together with the optimization of model parameterisations, such as deposition and chemical reactions, will lead to increasingly consistent long-term reanalyses in the future.

1 Introduction

Both human activity and natural processes influence the global distribution of present-day tropospheric ozone, together with its interannual variability and trends. Amongst other factors, increments in surface ozone concentrations contribute to changes in air quality (e.g., Im et al., 2018), human health (Liang et al., 2018), and agriculture (van Dingenen et al., 2009). Owing to its radiative effects, tropospheric ozone is an important driver in climate change (Checa-Garcia et al., 2018). Also it may affect long-range weather forecasts, even if in evaluations no improvement has been detected so far (Cheung et al., 2014). Considering its lifetime of a few weeks, tropospheric ozone can be controlled by both local and remote pollution sources through atmospheric chemical processes and long-range transport (Monks et al., 2015; Huang et al., 2017; Jonson et al., 2018), as well as stratospheric influx (e.g. Hsu and Prather, 2009; Knowland et al., 2017). In addition to anthropogenic sources, natural processes such as El Niño–Southern Oscillation (ENSO) conditions affect tropospheric ozone production and loss terms, through changes in upwelling, convection, solar irradiance, humidity, and biomass burning emissions (e.g., Ziemke and Chandra, 2003, Inness et al., 2015). Other processes that potentially influence tropospheric ozone, which is

generally considered of minor importance, are the quasi-biennial oscillation (Neu et al., 2014) and the North Atlantic Oscillation (Thouret et al., 2006).

Various types of datasets have been compiled to allow the analysis of the current state of tropospheric ozone and its changes over time. Surface ozone is reasonably well monitored through in-situ networks measuring surface concentrations (Global Atmosphere Watch (GAW), Global Monitoring Division (GMD), European Monitoring and Evaluation Programme (EMEP), AirNow), as collected and homogenised by the Tropospheric Ozone Assessment Report (TOAR, Schultz et al., 2017). Above the ground ozone is monitored through ozone sondes, collected by World Ozone and Ultraviolet Radiation Data Centre (WOUDC; https://woudc.org/), and aircraft (In-Service Aircraft for a Global Observing System (IAGOS), Nédélec et al., 2015). These observations are complemented with (combined) satellite observations from instruments such as Global Ozone Monitoring Experiment–2 (GOME-2), Ozone Monitoring Instrument (OMI), Microwave Limb Sounder (MLS), Infrared Atmospheric Sounding Interferometer (IASI), Tropospheric Emission Spectrometer (TES). Here each retrieval product comes with its specific (vertical) sensitivity, which allows the derivation of tropospheric ozone columns as listed in Gaudel et al. (2018).

The multitude of observational datasets have led to observationally constrained assessments of the current state and trends in tropospheric ozone, for instance documented as part of TOAR (Schultz et al., 2017; Gaudel et al., 2018; Fleming et al., 2018; Tarasick et al., 2019). Recent studies have also shown decadal-scale changes in global tropospheric ozone using various observations, such as a shift in the seasonal cycle at northern hemisphere (NH) mid-latitudes and long-term trends over many regions (e.g., Parrish et al., 2014; Cooper et al., 2014; Gaudel et al., 2018; Fleming et al., 2018). Based on a combination of multiple ozone retrieval products, Ziemke et al. (2019) have inferred positive trends in tropospheric ozone trends, particularly in the 2005-2016 time period.

Additional coordination with the emphasis on modelling activities related to tropospheric ozone have been established, for instance to analyse the contribution of ozone on air quality (AQMEII: Air Quality Modelling Evaluation International Initiative), the impact of long-range transport on air quality (HTAP: Hemispheric Transport of Air Pollution), and the impact of composition changes on climate change (CCMI: Chemistry-Climate Model Initiative). (e.g., Young et al., 2013; Morgenstern et al., 2018; Liang et al., 2018)

Following the concept of meteorological reanalyses such as ERA5 (Hersbach et al., 2018), observationally constrained reanalyses of the atmospheric chemical composition have been developed to provide time series of tropospheric and stratospheric ozone. A reanalysis is a systematic approach to create long-term data assimilation products by combining a series of observational datasets with a model. Advanced data assimilation, such as four-dimensional variational data assimilation (4D-VAR) and ensemble Kalman filter (EnKF), allows the propagation of observational information in time and space, and from a limited number of observed species, to an analysis of a wide range of chemical components. This can be used in reanalyses to provide consistent global fields that are in agreement with individual observations (Lahoz and Schneider, 2014; Bocquet et al., 2015). A reanalysis hence provides an instantaneous global image of atmospheric composition, together with its change over time and therefore serves in principle to analyse the mean state of the atmosphere, together with its variability and trends.

Applications of chemical reanalyses include comprehensive spatiotemporal evaluation of independent models, such as those developed in the framework of the Atmospheric Chemistry and Climate Model Intercomparison Project (ACCMIP, Young et al., 2013) and CCMI (Morgenstern et al., 2018). This was shown useful as evaluations using individual measurements are subject to significant sampling biases (Miyazaki and Bowman, 2017). In their study the ACCMIP ensemble ozone simulations were evaluated using a chemical reanalysis, complementing the use of individual measurements for such purpose. The chemical reanalyses can also be used as an input to meteorological reanalyses, e.g. for radiation calculations (Dragani et al., 2018), and they can provide boundary conditions to regional-scale models and to analyse particular pollution events such as those associated with heat waves or large-scale forest fires; Ordóñez et al., (2010), Huijnen et al., (2012,

2016). Finally, they can be used as a reference to identify to what extent particular periods and regions deviate from climatology, as provided by the reanalysis, as for instance also discussed in the series of the State of the Climate (Flemming and Inness, 2018).

However, all of these applications presume that the reanalysis is sufficiently accurate, or, to the least, well described. Despite the range of observations assimilated into the respective systems, this is not necessarily ensured. Issues are multiple, and depend on the availability of observations, and on the modelling and data-assimilation framework with respect to the species and location under consideration. For tropospheric ozone reanalyses, state-of-the-art global analysis systems have been used to assimilate satellite-based observations, where satellite measurements have limited information on vertical profiles. In particular, the small measurement sensitivities to the lower troposphere makes it difficult to correct near-surface ozone. Advanced satellite retrievals provide improved vertical resolution to the troposphere (Cuesta et al., 2018; Fu et al., 2018), but the temporal coverage and vertical resolution of these retrievals is still limited, and their application in data assimilation remains a challenge (Miyazaki et al., 2019a). This also implies that constraints on other parts of the system (other trace gases, aerosol, their emissions, as well as meteorology, driving the tracer transport and its removal) will strongly affect the quality of the reanalysis. Simultaneous optimization of concentrations and precursors' emissions seems thus important in improving the analysis of lower tropospheric ozone (Miyazaki et al., 2012b). Furthermore, providing consistent time series over a decadal time-scales is challenging. The observational data from satellite instruments available for assimilation evolve over time with new instruments becoming available while others cease to exist, and different satellite retrieval products typically showing biases with respect to ground-based observations as well as with respect to each other.

In the framework of the Copernicus Atmosphere Monitoring Service (CAMS, https://atmosphere.copernicus.eu), ECMWF's Integrated Forecasting System (IFS) has been extended to include modules for atmospheric chemistry, aerosols and greenhouse gases. Using this system, three recent reanalyses have been released: the Monitoring Atmospheric Composition and Climate (MACC) reanalysis for the years 2003-2012 (Inness et al., 2015), the 'CAMS Interim Reanalysis' (hereafter 'CAMS-iRean') for the years 2003-2018 (Flemming et al., 2017) and recently the 'CAMS Reanalysis' ('CAMS-Rean') for the years 2003-present (Inness et al., 2019). Miyazaki et al. (2015) simultaneously estimated concentrations and emissions for an 8-year tropospheric chemistry reanalysis (TCR-1) for the years 2005–2012 obtained from an assimilation of multi-constituent satellite measurements using an ensemble Kalman filter (EnKF). TCR-1 has been used to provide comprehensive information on atmospheric composition variability and elucidate variations in precursor emissions, and to evaluate bottom-up emission inventories (Miyazaki et al., 2012, 2014, 2015, 2017; Ding et al., 2017; Jiang et al., 2019; Tang et al., 2019). A second version of the EnKF-based reanalysis (TCR-2) has been recently produced using an updated model and satellite retrievals for the years 2005–2018 (Kanaya et al., 2019; Miyazaki et al., 2019a; Thompson et al., 2019). For stratospheric constituents, several studies have been conducted to produce and compare stratospheric chemical reanalysis products (Davis et al., 2017; Errera et al., 2019).

Here we evaluate the ability of the two CAMS and two TCR atmospheric composition reanalysis data sets to constrain tropospheric ozone variability. We do not evaluate the MACC reanalysis here, because it has been extensively documented in the past (Inness et al. 2013; Flemming et al., 2017; Bennouna et al., 2019) and only covered the 2003-2012 time period. Furthermore it has been shown to suffer from significant spurious drifts in tropospheric ozone due to a bias-correction issue, which makes it less useful to assess its multiannual mean and inter-annual variability. In particular, Katragkou et al. (2015) discusses the ozone in the MACC reanalysis; while Inness et al., (2019) reports how CAMS-Rean compares to CAMS-iRean and MACC reanalysis.

To assess the quality of these reanalysis products, with attention for the various potential types of application described above, this study evaluates tropospheric ozone for a range of independent in-situ observations: ozone sondes from networks World Ozone and Ultraviolet Radiation Data Centre (WOUDC), NOAA Earth System Research Laboratory (ESRL), and

Southern Hemisphere Additional Ozonesondes (SHADOZ), monthly mean gridded surface ozone as collected within TOAR, and individual surface ozone observations from the EMEP network.

In this study, we limit ourselves to tropospheric ozone in the reanalysis products, and only refer, where relevant, to interactions with other components in the reanalysis systems, such as nitrogen oxides (NO_x) and carbon monoxide (CO), and aerosols. Even though these four reanalysis products are not equally independent, each of their configurations show substantial differences which are bound to impact the performance of the reanalysis products. This intercomparison aims to reveal to what extend the reanalysis products agree, depending on region and time periods. Temporal consistency is an important aspect when assessing long-term time series and intercomparing individual years. At the same time this is a challenge because of the change in the observing system used to constrain the reanalysis products over the course of a decade or more, all having different retrieval specifications (see also Gaudel et al., 2018).

In the next sections we describe the various reanalysis products used in this paper (Sect. 2) and the observational data used for evaluation (Sect. 3). Evaluations against ozone sondes are presented in Sect. 4, and against TOAR gridded surface ozone and EMEP surface observations in Sect. 5, and Sect. 6, respectively. We continue describing the reanalysis products through assessment of their global spatial and temporal consistency (Sect 7). We end with discussions and conclusions in Sect 8.

2. Chemical reanalysis products

The global atmospheric chemistry reanalysis products evaluated in this paper are listed in Table 1. The general configuration of the various data assimilation systems, together with details specific to tropospheric ozone analysis, are provided in the following subsections. For more detailed information on the specifications of the various reanalysis products the reader is referred to the references.

Table 1. Overview of recent reanalysis products

Name (reference)	Time period	Altitude range and horizontal resolution	Forecast model	Data assimilation scheme	Assimilated components
CAMS-iRean (Flemming et al., 2017)	2003-2018	Up to 0.1hPa T159/L60	IFS(CB05) CY40R2	4D-VAR	CO, O_3, AOD
CAMS-Rean (Inness et al., 2019)	2003-present	Up to 0.1hPa T255/L60	IFS(CB05) CY42R1	4D-VAR	CO, O_3, NO_2, AOD
TCR-1 (Miyazaki et al., 2015; Miyazaki et al., 2017; Miyazaki and Bowman, 2017)	2005-2014	Up to 4.4 hPa T42/L32	MIROC-Chem Nudged to ERA-Interim	EnKF	CO, O_3, NO_2, HNO_3
TCR-2 (Miyazaki et al., 2019a, Kanaya et al., 2019)	2005-2018	Up to 4.4 hPa T106/L32	MIROC-Chem Nudged to ERA-Interim	EnKF	CO, O_3, NO_2, HNO_3, SO_2

2.1 The CAMS Interim reanalysis

In CAMS, the data assimilation capabilities in IFS for trace gases and aerosols relies on the four-dimensional variational (4D-VAR) technique, developed for the analysis of meteorological fields. The CAMS interim Reanalysis (CAMS-iRean, Flemming et al., 2017) has been the intermediate reanalysis between the widely used MACC Reanalysis (Inness et al., 2015) and the recently produced CAMS reanalysis (Inness et al., 2019). The chemistry module as adopted in CAMS-iRean is described and evaluated in Flemming et al. (2015). It relies on the modified CB05 tropospheric chemistry mechanism as originating from TM5 (Huijnen et al., 2010; Williams et al., 2013) which contains 52 species and 130 (gas-phase + photolytic) reactions; stratospheric ozone is modelled through the Cariolle parameterization (Cariolle and Teyssèdre, 2007). Anthropogenic emissions originate essentially from the MACCity inventory (Granier et al., 2011) with enhanced wintertime CO emissions over Europe and US (Stein et al., 2014). Monthly specific biogenic emissions originate from MEGAN-MACC (Sindelarova et al., 2014), but using monthly climatological values from 2011 onwards. Daily biomass burning emissions originate from GFASv1.2 (Kaiser et al., 2013). The meteorological model is IFS CY40R2.

In terms of ozone, observations from the following set of satellite instruments have been assimilated: Solar Backscatter ULTa-Violet (SBUV/2), OMI, MLS, GOME-2, SCanning Imaging Absorption spectroMeter for Atmospheric CHartographY (SCIAMACHY), GOME and Michelson Interferometer for Passive Atmospheric Sounding (MIPAS), see also Table 2. A variational bias correction (VarBC) scheme was applied to OMI, SCIAMACHY and GOME-2 retrievals of total ozone columns to ensure optimal consistency of all information used in the analysis. SBUV/2 and also profile retrievals from MLS and MIPAS were assimilated without correction. Note that no total columns are assimilated for solar elevations less than 6°, hence excluding polar winters.

Profile observations from limb instruments in the range of 0.1-150 hPa for MIPAS and 0.1-147 hPa for MLS are used to constrain the stratospheric contribution of the total column. In combination with the assimilated total column retrievals this implies that also the tropospheric part is constrained (Inness et al., 2013). CAMS-iRean uses observations from the MIPAS instrument for the period February 2005 - March 2012. MLS data on Aura have been used from August 2004 onwards, based on version 2 observations during August 2004-Dec 2012, and V3.4 from January 2013 onwards. V3.4 has a different specification of the vertical levels and observation errors compared to V2 (Schwartz et al., 2015 and https://mls.jpl.nasa.gov/data/v3_data_quality_document.pdf). Finally, note that in CAMS-iRean no observations of NO_2 have been assimilated. CO has been constrained through assimilation of Measurement of Pollution in the Troposphere (MOPITT) total columns.

180   **Table 2: Observations of ozone used in the CAMS-iRean assimilation system**

Instrument (satellite)	Product	Data provider/version	Period	Reference
SCIAMACHY (Envisat)	TC	ESA / CCI (TC_SCIAMACHY/fv0300)	2003-01-01 to 2012-04-08	Lerot et al. (2009)
MIPAS (Envisat)	Prof	ESA / NRT ESA CCI (HARMOZ_MIPAS)/fv0004	2005-01-27 to 2012-03-31	Von Clarmann et al. (2003, 2009)
MLS (Aura)	Prof	NASA /V2 NASA/V3.4	2004-08-03 to 2012-12-31 2013-01-01 to 2016-12-31	Schwartz et al. (2015)
OMI(Aura)	TC	KNMI /V3 KNMI /NRT	2004-08-03 to 2015-05-31 2015-06-01 to present	Liu et al. (2010)
GOME (ERS-2)	Prof	RAL	2003-01-01 to 2003-05-31	Munro et al. (1998)
GOME-2 (Metop-A)	TC	ESA, CCI /fv0100 ESA, CCI /fv0300 NRT	2007-01-23 to 2012-12-31 2013-01-01 to 2016-12-31 2017-01-01 to present	Hao et al. (2014)
GOME-2 (Metop-B)	TC	ESA, CCI /fv0300 NRT	2013-01-01 to 2016-12-31 2017-01-01 to present	Hao et al. (2014)
SBUV/2 (NOAA-14 – NOAA-19)	PC	NASA / v8.6 13L NRT 21L	2003-01-01 to 2012-12-31 2013-01-01 to present	Bhartia et al. (1996), McPeters et al. (2013)

185

Table 3: Observations of ozone used in the CAMS-Rean assimilation system

Instrument (satellite)	Product	Data provider/version	Period	Reference
SCIAMACHY (Envisat)	TC	ESA, CCI (TC_SCIAMACHY/fv0300)	2003-01-01 to 2012-04-08	Lerot et al. (2009)
MIPAS (Envisat)	Prof	ESA, NRT ESA, CCI (HARMOZ_MIPAS)/fv0004	2003-01-27 to 2004-03-26 and 2005-01-27 to 2012-03-31	Von Clarmann et al. (2003, 2009)
MLS (Aura)	Prof	NASA /V4	2004-08-03 to 2016-12-31	Schwartz et al. (2015)
OMI(Aura)	TC	KNMI /V3 KNMI /NRT	2004-08-03 to 2015-05-31 2015-06-01 to present	Liu et al. (2010)
GOME-2 (Metop-A)	TC	ESA, CCI /fv0100 ESA, CCI /fv0300 NRT	2007-01-23 to 2012-12-31 2013-01-01 to 2016-12-31 2017-01-01 to present	Hao et al. (2014)
GOME-2 (Metop-B)	TC	ESA, CCI /fv0300 NRT	2013-01-01 to 2016-12-31 2017-01-01 to present	Hao et al. (2014)
SBUV/2 (NOAA-14 – NOAA-19)	PC	NASA / v8.6 13L NRT 21L	2003-01-01 to 2013-07-07 2013-07-08 to present	Bhartia et al. (1996), McPeters et al. (2013)

2.2 The CAMS Reanalysis

The CAMS Reanalysis (CAMS-Rean; Inness et al., 2019) is the successor of the CAMS-iRean. Compared to CAMS-iRean,
190   the horizontal resolution has increased to ~80 km (T255), while meteorology is now based on CY42R1. Emissions are largely similar to CAMS-iRean, except that the monthly varying biogenic emissions have been used for the full time period. With respect to the CB05-based chemistry module, heterogeneous chemistry on clouds and aerosol has been switched on, as well as the modification of photolysis rates due to aerosol scattering and absorption (Huijnen et al., 2014).

As for assimilated ozone observations, data from a very similar set of instruments have been used as for CAMS-iRean:
195   SCIAMACHY, MIPAS, OMI, MLS, GOME-2, and SBUV/2, see Table 3. However, note that the CAMS-Interim Reanalysis additionally assimilated GOME profile observations during the first 5 months of 2003, which have not been assimilated in CAMS-Rean as it was found to lead to a degradation in the O_3 analysis. Different to CAMS-iRean, CAMS-Rean also assimilated observations from the MIPAS instrument during 2003 and early 2004, although using a different version. Also frequently newer versions of the data have been adopted in CAMS-Rean compared to CAMS-iRean, particularly for MLS
200   observations the reprocessed version 4 has been applied throughout the full time period.

In CAMS-Rean also tropospheric NO_2 columns are assimilated, using observations from the SCIAMACHY (2003-2012), OMI (from October 2004 onwards) and GOME-2 (from April 2007 onwards) instruments. The same settings for the variational bias correction were used in CAMS-Rean as in CAMS-iRean.
205   CAMS-iRean and CAMS-Rean surface and tropospheric ozone are archived with a three-hourly output frequency.

2.3 Tropospheric Chemistry Reanalysis (TCR-1)

The TCR-1 data assimilation system is constructed using an EnKF approach. A revised version of the TCR-1 data is used in this study. A major update from the original TCR-1 system (Miyazaki et al., 2015) to the system used here (Miyazaki et al.,

2017; Miyazaki and Bowman, 2017) is the replacement of the forecast model from CHASER (Sudo et al., 2002) to MIROC-Chem (Watanabe et al., 2011), which caused substantial changes in the a priori field and thus the data assimilation results of various species.

MIROC-Chem considers detailed photochemistry in the troposphere and stratosphere by simulating tracer transport, wet and dry deposition, and emissions, and calculates the concentrations of 92 chemical species and 262 chemical reactions. The MIROC-Chem model used in TCR-1 has a T42 horizontal resolution (~2.8°) with 32 vertical levels from the surface to 4.4 hPa. It is coupled to the atmospheric general circulation model MIROC-AGCM version 4 (Watanabe et al., 2011). The simulated meteorological fields were nudged toward the 6-hourly ERA-Interim (Dee et al., 2011) to reproduce past meteorological fields.

The a priori anthropogenic NO_x and CO emissions were obtained from the Emission Database for Global Atmospheric Research (EDGAR) version 4.2 (EC-JRC, 2011). Emissions from biomass burning were based on the monthly Global Fire Emissions Database (GFED) version 3.1 (van der Werf et al., 2010). Emissions from soils were based on monthly mean Global Emissions Inventory Activity (GEIA; Graedel et al., 1993).

The data assimilation used is based upon on an EnKF approach (Hunt et al., 2007) that uses an ensemble forecast to estimate the background error covariance matrix and generates an analysis ensemble mean and covariance that satisfy the Kalman filter equations for linear models. The concentrations and emission fields of various species are simultaneously optimized using the EnKF data assimilation, see also Table 4.

For data assimilation of tropospheric NO_2 column retrievals, the version 2 Dutch OMI NO_2 (DOMINO) data product (Boersma et al., 2011) and version 2.3 TM4NO2A data products for SCIAMACHY and GOME-2 (Boersma et al., 2004) were used, obtained through the TEMIS website (http://www.temis.nl). The TES ozone data and observation operators used are version 5 level 2 nadir data obtained from the global survey mode (Bowman et al., 2006; Herman and Kulawik, 2013). TES ozone data was excluded poleward of 72 degree because of the small retrieval sensitivity, limiting data assimilation adjustments at high latitudes in the troposphere. Also note that the availability of TES measurements is strongly reduced after 2010, which led to a degradation of the reanalysis performance, as demonstrated by Miyazaki et al. (2015). The MLS data used are the version 4.2 ozone and HNO_3 level 2 products (Livesey et al., 2018). Data for pressures of less than 215 hPa for ozone and 150 hPa for HNO_3 were used. The MOPITT CO data used are version 6 level 2 thermal-infrared retrieval (TIR) products (Deeter et al., 2013). A superobservation approach was employed to produce representative data with a horizontal resolution of the forecast model NO_2 and CO observations, following the approach of Miyazaki et al. (2012). No bias correction was applied to the assimilated measurements.

2.4 Updated Tropospheric Chemistry Reanalysis (TCR-2)

An updated Chemistry Transport Model (CTM) and satellite retrievals are used in TCR-2 (Kanaya et al., 2019; Miyazaki et al., 2019a, 2019b; Thompson et al., 2019). A high-resolution version of the MIROC-Chem model with a horizontal resolution of T106 (1.1° x 1.1°) was used. Sekiya et al. (2018) demonstrated the improved model performance on tropospheric ozone and its precursors by increasing the model resolution from 2.8° x 2.8° to 1.1° x 1.1°. A priori anthropogenic emissions of NO_x and CO were obtained from the HTAP version 2 inventory for 2008 and 2010 (Janssens-Maenhout et al., 2015). Emissions from biomass burning are based on the monthly GFED version 4.2 inventory (Randerson et al., 2018) for NO_x and CO, while those from soils are based on the monthly GEIA inventory (Graedel et al., 1993) for NO_x. Emission data for other compounds are taken from the HTAP version 2 and GFED version 4 inventories.

The satellite products used in TCR-2 are more recent than those used in TCR-1, see Table 4. Tropospheric NO_2 column retrievals used are the QA4ECV version 1.1 L2 product for OMI (Boersma et al., 2017a) and GOME-2 (Boersma et al., 2017b). Version 6 of the TES ozone profile data was used. The MLS data used are the version 4.2 ozone and HNO_3 L2

products (Livesey et al., 2018). The MOPITT total column CO data used were the version 7L2 TIR/NIR product (Deeter et al., 2017). OMI SO_2 data of the planetary boundary layer vertical column L2 product were used as produced with the principal component analysis algorithm (Krotkov et al., 2016; Li et al., 2013). As in TCR-1, a super-observation approach to produce representative data with a horizontal resolution of the forecast model (1.1° × 1.1°) for NO_2 and CO observations was applied. As in TCR-1, no bias correction was applied to the assimilated measurements.

TCR-2 data was used to study the processes controlling air quality in East Asia during the KORUS-AQ aircraft campaign (Miyazaki et al., 2019a). Kanaya et al. (2019) demonstrated the TCR-2 ozone and CO performance using research vessel observations over open oceans. Thompson et al. (2019) used the TCR-2 data to help understanding of near surface NO_2 pollutions observed during the KORUS-OC campaign. Both for TCR-1 and TCR-2 the reanalysis data is archived on a two-hourly output frequency.

Table 4: Observations used for ozone assimilation in TCR-1, and in square brackets changes for TCR-2.

Instrument (satellite)	Species	Product	Data provider/version	Period	Reference
OMI (Aura)	NO_2 [+ SO_2]	TrC for NO_2 [PBL for SO_2]	DOMINO v2 [QA4ECV v1.1] for NO_2 [PCA v3 for SO_2]	2005-01-01 to present	Boersma et al. (2011) [Boersma et al. (2017a)] [Krotkov et al. (2016); Li et al. (2013)]
SCIAMACHY (Envisat)	NO_2	TrC	DOMINO v2 [QA4ECV]	2005-01-01 to 2012-03-29	Boersma et al. (2004) [(Boersma et al. (2017b)]
GOME-2 (Metop-A)	NO_2	TrC	DOMINO v2 [QA4ECV]	2007-01-01 to present	Boersma et al. (2004) [(Boersma et al. (2017b)]
TES (Aura)	O_3	Profile	v5 [v6]	2005-01-01 to 2011-06-04	Bowman et al. (2006); Herman and Kulawik (2013)
MLS (Aura)	O_3, HNO_3	Profile	v4.2 [v4.2]	2005-01-01 to present	Livesey et al. (2018)
MOPITT (Terra)	CO	Profile	v6 NIR [v7 TIR/NIR]	2005-01-01 to present	Deeter et al. (2013) [Deeter et al. (2017)]

2.5 Temporal consistency of the observing systems

Discontinuities in the observing systems, as specified in Tables 2-4, can cause significant temporal changes in the reanalyses quality. In 4D-Var systems this can be assessed through statistics based on analysis departures (observation minus analysis) and first guess departures (observations minus model first guess). Inness et al. (2019) provide an extended overview of the biases of various assimilated observations against the CAMS Reanalysis. For ozone assimilation in particular, the following findings are most noteworthy for this study (see also Appendix C of Inness et al., 2019):

•	Larger biases for SCIAMACHY observations in 2003 and early 2004, associated to issues with the early SCIAMACHY O_3 retrievals in this time period

- Larger departures for MIPAS data during 2003-2004 than after 2005, where CCI data was used

- Different behaviour of OMI data between 2009 and 2012, associated to a deterioration in the OMI row anomalies (Schenkeveld et al., 2017) which unfortunately have not be filtered out in the CAMS assimilation procedure.

- An increasing bias correction for GOME-2A especially after January 2013, associated to a version change of the SBUV/2 data.

With respect to both TCR reanalyses which are based on the EnKF approach, important information regarding the reanalysis product is provided by the error covariance. The analysis ensemble spread is estimated as the standard deviation of the simulated concentrations across the ensemble and can be used as a measure of the uncertainty of the reanalysis product (Miyazaki et al., 2012). The uncertainty information on the analysis uncertainty is included in the TCR-1 and TCR-2 reanalysis products and this can be used to investigate the long-term stability of the data assimilation performance. In addition, the χ^2 test was used to evaluate the temporal changes in data assimilation balance (e.g. Ménard and Chang, 2000). Miyazaki et al (2015) demonstrated increased χ^2 for OMI NO$_2$ after 2010, associated with a decrease in the number of the assimilated measurements and changes in the super-observation error due to the OMI row anomalies. Furthermore, the decreased number of assimilated TES ozone retrievals after 2010 affected the long-term reanalysis characteristics. Before 2011 the analysis spread for ozone in the middle troposphere is about 1-3 ppb in the tropics and subtropics and 3-12 ppbv in the extratropics. The larger spread at lower latitudes could be attributed to the higher sensitivities in the TES ozone retrievals. From 2011 onwards the spread mostly becomes smaller than 3 ppb for the globe, which seems excessively small and is likely associated with the lack of effective observations for measuring the analysis uncertainties and with the stiff tropospheric chemical system. The obtained results indicate the requirements for additional observational information and/or stronger covariance inflation to the forecast error covariance for measuring the long-term analysis spread corresponding to actual analysis uncertainty.

3. Ozone observations used for evaluation

3.1 Ozone sondes

For evaluation of free tropospheric ozone data from the global network of ozone sondes, as collected by the WOUDC, is used, expanded with observations available from SHADOZ (Thompson et al., 2017; Witte et al., 2017) and ESRL. The observation error of the sondes is about 7–17% below 200 hPa and ±5% in the range between 200 and 10 hPa (Beekmann et al., 1994, Komhyr et al., 1995 and Steinbrecht et al., 1996). Typically, the sondes are launched once a week, but in certain periods, such as during ozone hole conditions, launches can be more frequent. Sonde launches are mostly carried out between 9:00 and 12:00 local time.

The ozone sonde network provides critical independent validation of the reanalysis products. Although the number of soundings varied for the different stations, the global distribution of the launch sites is expected to be sufficient to allow meaningful monthly to seasonal averages over larger areas. However, because of the sparseness of the ozone sonde network, we are aware that the evaluation based on ozone sonde observations can introduce large biases in regional and seasonal reanalysis performance (Miyazaki and Bowman, 2017).

The reanalysis data have been collocated with observations through interpolation in time and space. Individual intercomparisons have been aggregated on a monthly and seasonal basis. The number of stations contributing to the monthly and regional means varies over the course of the reanalysis products, and is additionally reported as this is naturally an important consideration when assessing interannual variability of ozone biases. While we present time series from 2003 onwards in our figures, where CAMS starts to provide reanalysis products, for any of the statistics we only base this on the 2005-2016 time period (unless explicitly mentioned), to allow fair intercomparison between CAMS and TCR.
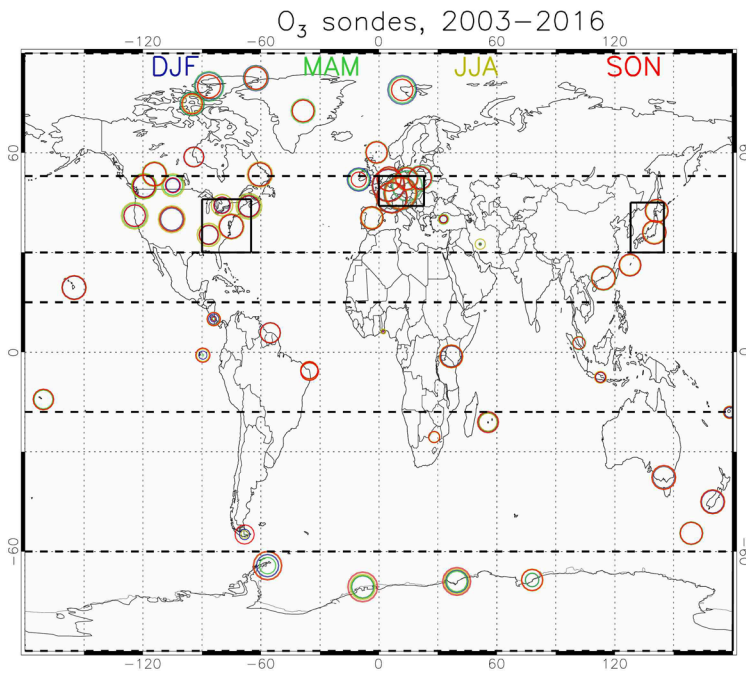
Figure 1: Location of ozone sondes contributing to the various regions. The size of circles indicates the relative number of observations contributing to the statistics for December–February (blue), March–May (green), June–August (yellow), and September–November (red). The dashed lines indicate the latitude bands representing the NH arctic region (53°N-90°N), NH mid latitudes (30°N -53°N), NH subtropics (15°N-30°N), Tropics (18°S-15°N), SH mid latitudes (60°S-18°S) and Antarctic (90°S-60°S). The black boxes indicate three additional regions in the NH-mid latitudes: Eastern US (90°W-65°W, 30°N-46°N), Western Europe (0°E-23°E), Japan (30°N-45°N, 128°E-145°E).

For spatial aggregation the choice is more difficult, depending on the characteristics of the species and availability of observations. Tilmes et al. (2012) defined an aggregation approach for ozonesonde locations based on the characteristics of the observed ozone profiles. We follow in part their aggregation approach, by adopting the European, Eastern US, Japan, and Antarctic regions. For several regions, the number of measurements could be insufficient to construct meaningful aggregates. Instead we define regions for the northern hemisphere (NH) subtropics, the tropics, southern hemisphere (SH) mid latitudes and Antarctic, and combine the NH Polar regions to a single region, see also Figure 1.

3.2 Surface ozone

We evaluate surface ozone against the TOAR database (Schultz et al., 2017), which provides a globally consistent, gridded, long-term dataset with ozone observation statistics on a monthly mean basis. The TOAR database has been produced with particular attention to quality control, and representativeness of the in-situ observations, in order to establish consistent, long-term time records of observations. TOAR provides a disaggregation of rural and urban stations. For our study we use the 2°×2° gridded monthly mean dataset representative for rural stations for the 1990-2014 time period. This allows easy intercomparison with monthly mean results from the various reanalysis products.

Note that in these comparisons we used rural observations only, because none of the reanalysis model resolutions is considered sufficient to resolve local concentration changes over highly polluted urban areas. Therefore the rural observations can be considered as more representative data for grid averaged concentrations. Nevertheless, neglecting urban observations could lead to biased evaluations particularly in cases where large fractions of the grid cells are associated to urban conditions, e.g. in megacities.

340 This TOAR dataset has a good global coverage, including stations over East Asia, and provides overall a constant, and good quality controlled data record up to 2014. Nevertheless, the number of records in this database decreases significantly for various regions on the globe after 2012. Therefore in our evaluation statistics we focus on the period before 2012, considering that the reduction in available observations afterwards hampers the intercomparison of reanalysis performance between different years. Similar to the evaluation against ozone sonde observations, the statistics is computed for data from

345 2005 onwards.

3.3 EMEP observations

In order to assess the ability of the reanalysis products to represent spatial and temporal variability on a sub-seasonal and on regional scales, we additionally evaluate the reanalyses against ground-based hourly observations from the EMEP network (obtained from http://ebas.nilu.no/) for the year 2006. Although EMEP data are also included in the TOAR data product, this

350 analysis allows for a complementary approach, in particular the assessment of pollution events during heat waves, but also evaluation of the diurnal cycles and spatial variability in the various products. The summer period of 2006 over Europe was characterized by a heat wave event (Struzewska and Kaminski, 2008). For this evaluation, we collocate the reanalysis output spatially and temporally to the observations, using a reference 3-hourly time frequency. Considering the comparatively coarse horizontal resolution, which is not generally able to represent the local orography at the location of the individual

355 observations, we match the model level with the same (average) pressure level at the location of the observations. Here we note that the CAMS reanalyses use a higher vertical resolution than TCR. This implies that for high-altitude stations also different (higher) model levels are sampled in the CAMS reanalyses compared with TCR. After this collocation procedure, we compute temporal correlation coefficients on a seasonal basis, using the temporally collocated 3-hourly reanalysis and observational data.

360 **4. Evaluation against ozonesondes**

4.1 Annually and regionally averaged profiles

Figure 2 provides an overview of the multiannual mean ozone for the four reanalyses for the 2005–2016 time period. All reanalyses capture the observed vertical profiles of ozone from the lower troposphere to the lower stratosphere, with a regional mean bias of typically less than 8 ppb throughout the troposphere. Corresponding mean biases at 850, 650 hPa and

365 350 hPa are given in Figure 3, where the bias is defined as the reanalysis-observation, throughout this work. The normalized values, as scaled with the mean of the observations, are given in Figure S1 in the Supplementary Material. These multiannual, regional mean biases are below 3.7 ppb at 850 hPa and 4 ppb at 650 hPa, while normalized (absolute) biases are mostly below 10%. For most regions, the CAMS reanalysis shows improvement against the CAMS interim reanalysis at 650 hPa and also 850 hPa, particularly for regions over the NH high- and mid-latitudes, as well as the SH-mid latitudes, but at

370 the cost of a degradation (an emerging positive bias) towards the surface. TCR-2 shows a more mixed picture in this respect. Biases between TCR and CAMS are within a similar order of magnitude, but are not correlated in any way in sign or magnitude. For most of the major polluted areas in the lower troposphere, the biases are lower in the CAMS reanalysis than in the TCR reanalyses, probably due to its higher reanalysis model resolution and a better chemical forecast model performance. The annual mean ozone biases in TCR are relatively large in the tropics and SH high latitudes. After 2011, no

375 TES tropospheric ozone measurements were assimilated, which could lead to enhanced ozone biases, as demonstrated by Miyazaki et al. (2015). Assimilation of MLS measurements does not noticeably influence the tropospheric ozone analysis in the tropics. In the NH subtropics and the tropics regions the reanalyses show some larger deviation against sonde observations at lower altitudes, which was traced to comparatively large biases at the Hong Kong and Kuala Lumpur stations. Note that in these regions the ozonesonde network is sparse, while the spatial and temporal variability of ozone is

380 large, which limits our understanding of the generalized reanalysis performance (Miyazaki and Bowman, 2017). At high latitudes, the large diversity in the reanalysis ozone could be associated with the lack of direct tropospheric ozone measurements in all of the systems.

Overall, this evaluation shows that the biases from these reanalysis products are smaller than those reported from recent CTM simulations. E.g. Young et al. (2013) present median biases across ACCMIP model versions at 700 (500) hPa up to 10 385 (15)%, depending on the region. This demonstrates that the reanalysis of tropospheric ozone fields is generally well constrained by assimilated measurements for the globe.
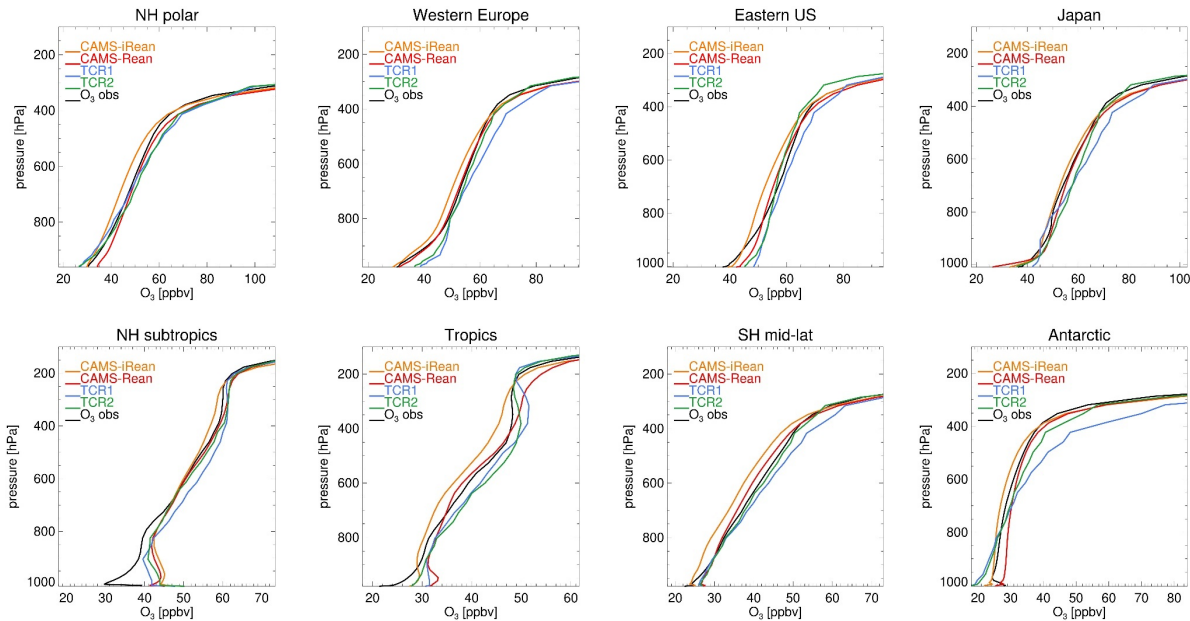
390 **Figure 2: Evaluation of regional mean multiannual mean O₃ profiles against ozone sondes, averaged over the 2005–2016 time period.**
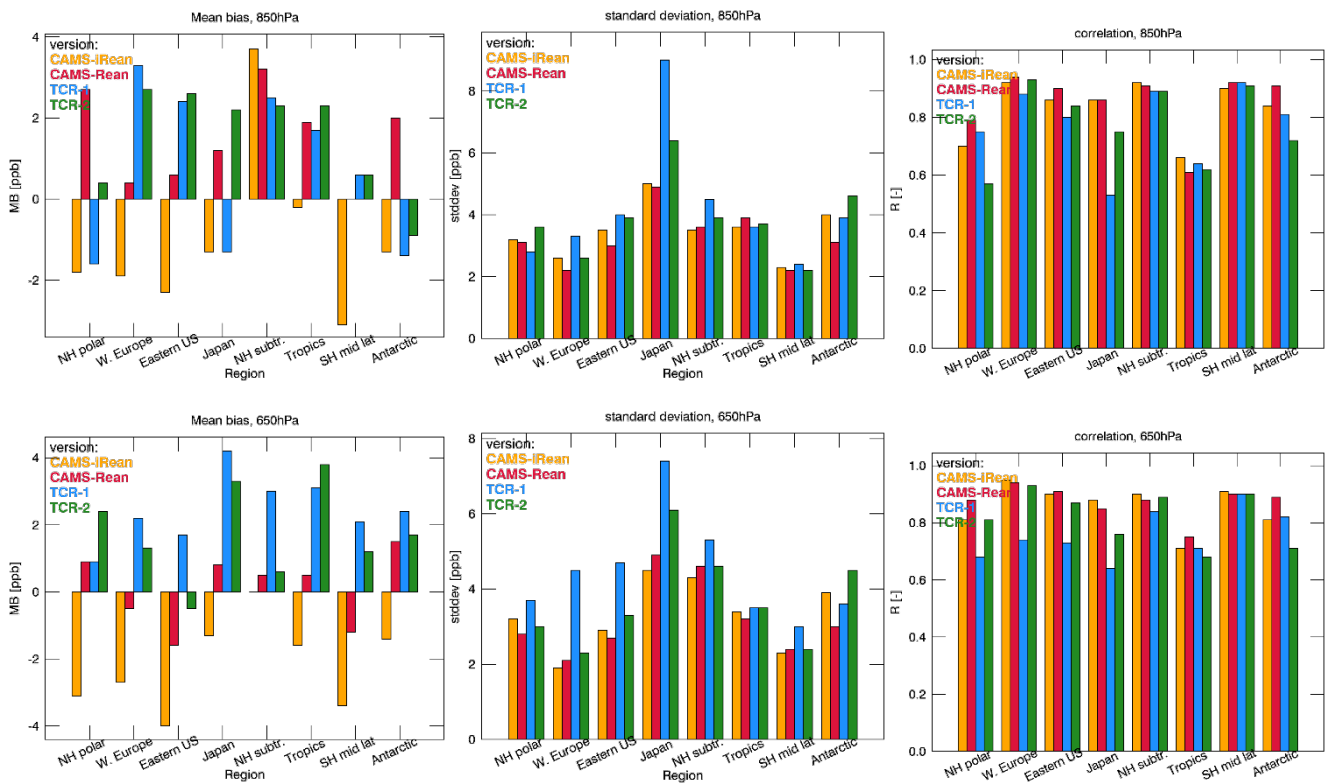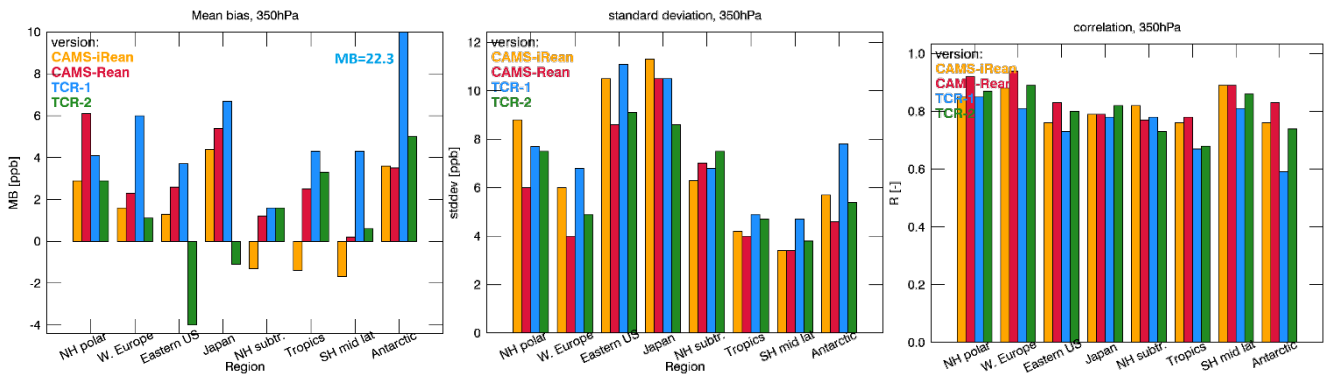
Figure 3: Evaluation of ozone mean bias (reanalysis-observation, left), standard deviation of the unbiased differences (middle) and temporal correlation R (right) for the four reanalysis products at 850 (top), 650 (middle) and 350 (bottom) hPa against sondes, computed for various regions, for the 2005-2016 time period.

4.2 Time series of zonally averaged O₃ tropospheric columns

Collocated partial columns from the surface up to 300 hPa, hereafter for brevity referred to as 'tropospheric columns', have been compared to partial columns derived from the sonde observations. An intercomparison of the monthly and zonally mean tropospheric columns sampled at the observations is given in Figure 4. The corresponding performance statistics is given in Figure 5. Here, the standard deviation (stddev) is computed based on the unbiased differences between the reanalyses and sonde observations, and provides a metric of the quality of the monthly mean variability in the reanalyses. Normalized statistics are provided in Figure S2 in the Supplementary Material. Note that the figures also contain information on the number of sonde stations that are included in the evaluation for individual months.

Outside the polar regions all reanalyses capture the magnitude of the zonal mean tropospheric column to within a MB of within 1.8 DU, and the stddev between 0.8 and 1.3 DU depending on the reanalysis product. For most regions and performance metrics, the updated reanalyses outperform their predecessor versions. For instance, for the NH mid latitudes the MB is -0.3 DU (1.2%, when normalized with sonde observations) for CAMS-Rean and 0.8 DU (3%) for TCR-2, which was earlier -1.2 DU (CAMS-iRean) and 1.8 DU (TCR-1).

Largest uncertainties are found for the polar regions, with MB within 2.6 DU and the stddev ranging between 1.4 (CAMS-Rean) to 2.1 (TCR-1) DU, corresponding to up to ~12% of the average O₃ tropospheric column. Over the SH mid latitudes the reanalyses show similar features as over the Antarctic, with normalized mean biases within -1DU (-5%, CAMS-iRean) and 1.5 DU (+10%, TCR-1). The normalized standard deviations over the SH mid latitudes are within 7%, marking a considerably better ability to capture temporal variability than over the Antarctic.

In the tropics the MB ranges within -0.6 to 1.2 DU, and the stddev is about 1.0DU, or ~5% of the average O₃ tropospheric column. The temporal correlation between analyzed and observed tropospheric columns is correspondingly highest (R>0.90) for the NH mid-latitudes, but still relatively low for the Antarctic region (R<0.80) for all reanalyses. This relatively poor temporal correlation over the Antarctic, despite the strong seasonal cycle, does indicate difficulties of the reanalyses to reproduce a consistent seasonality over the full time series, as described in more detail in the following sections.
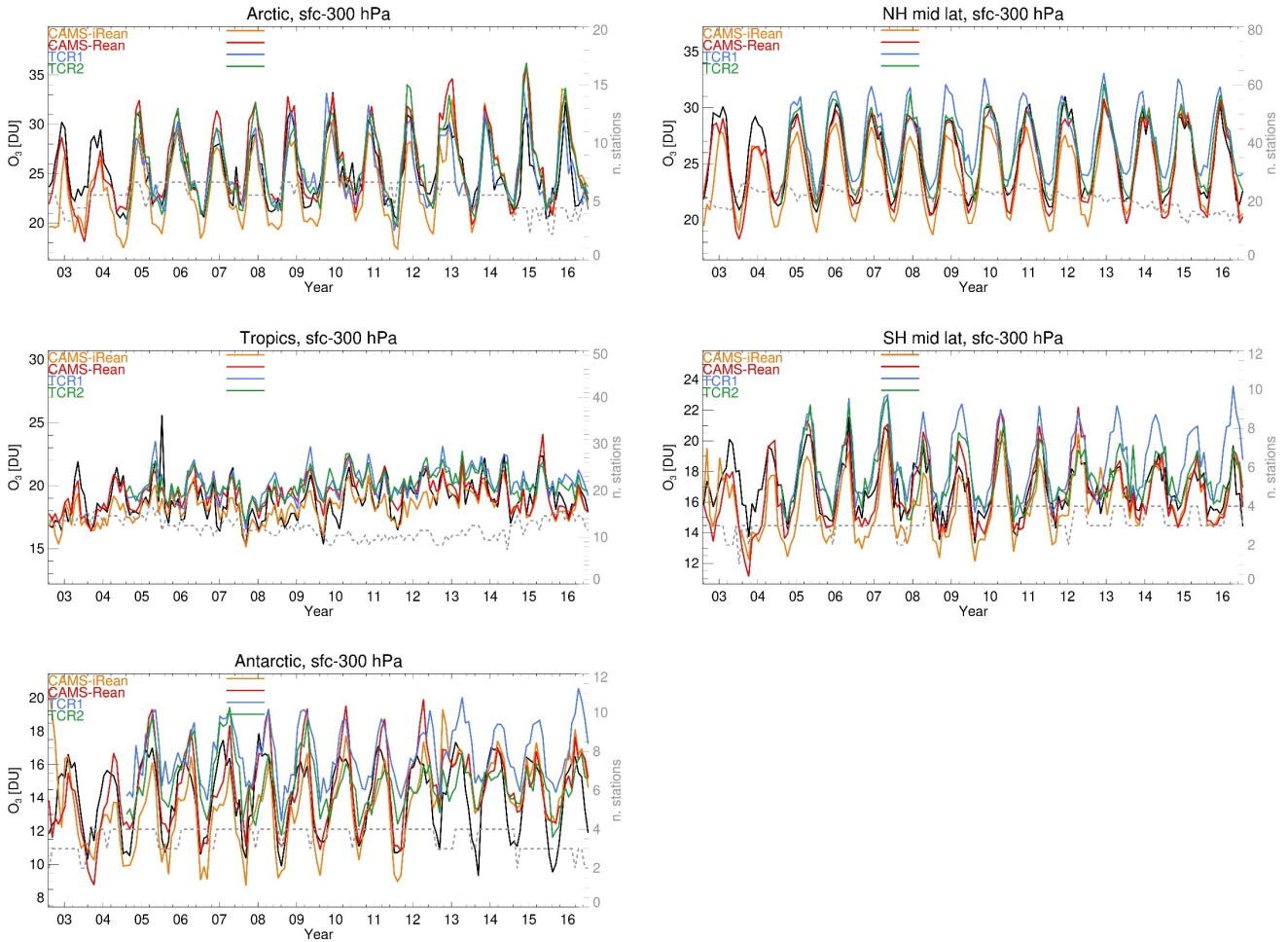
Figure 4: Evaluation of zonally averaged monthly mean partial columns (surface – 300 hPa) against sonde observations. Observations are in black. The gray dashed line refers to the number of stations that contribute to the statistics (right vertical axis).
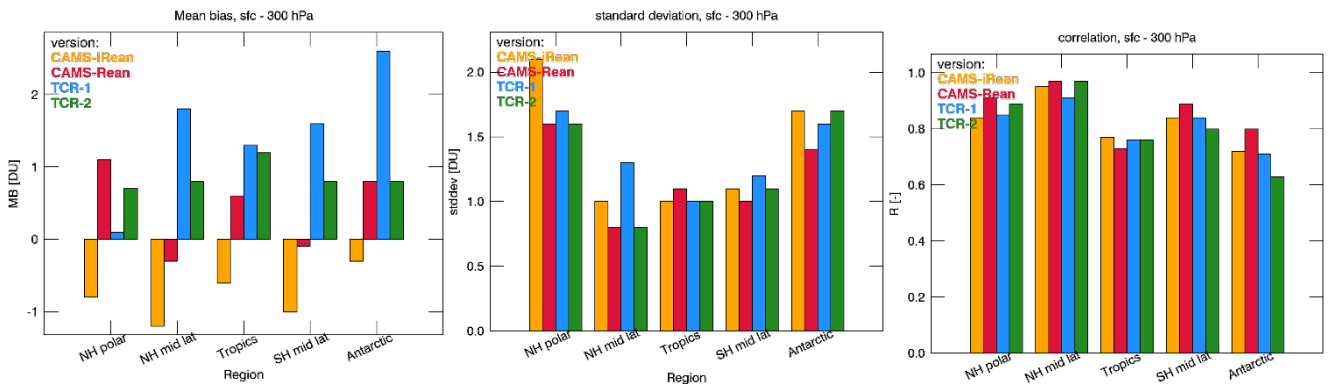
Figure 5. Analogous to Figure 3 but for partial columns from surface to 300hPa, in Dobson Units (DU).

4.3 Time series of regionally averaged O₃ biases at multiple altitudes

Figure 6 shows time series of monthly mean ozone biases against ozone sondes at three pressure levels (~850, 650, and 350 hPa), aggregated for the predefined regions. The panels in this figure give an indication of the stability of the reanalyses against sonde observations during the 2003–2016 time period. The corresponding timeseries with monthly mean

concentration values, showing the seasonal cycle, is given in Figure S3 in the Supplementary material. As in the previous section, persistent changes in the number of stations may contribute to changes in biases over the course of the fourteen year time interval. The mean bias, stddev and temporal correlation for each of these time series are given in Figure 3. Based on these evaluations we note the following: Over the **NH polar** region, CAMS-Rean shows a small positive bias in the lower troposphere (2.7 ppb at 850 hPa for the 2005-2016 multiannual mean), particularly during the springtime (5.0 ppb when averaged over March-May). During 2003 and 2004 both CAMS reanalyses show anomalously low springtime ozone, different to the rest of the time period, particularly at ~350 hPa. The different reanalysis performance statistics over the Arctic compared to later years is attributed to the use of early SCIAMACHY and NRT MIPAS O_3 retrievals, which are of poorer quality than the OMI MLS observations which have been used from August 2004 onwards, and reprocessed MIPAS data used from January 2005 onwards. Combined with total column retrievals, assimilation of such stratospheric profiles has been shown to also affect the tropospheric contribution (Inness et al., 2013). CAMS-iRean shows a large offset compared to observations and CAMS-Rean in 2003, particularly at altitudes below 650 hPa. This was attributed to the assimilation of GOME nadir profiles in CAMS-iRean, which has been omitted in CAMS-Rean (Inness et al., 2019).

Furthermore, before 2014 CAMS-iRean shows lower values than CAMS-Rean, while for 2014 to 2016 the two CAMS reanalyses are much more alike. This offset before 2014 results in a slight negative bias against observations at ~850 hPa over the Arctic, and a significant negative bias at ~650 hPa, and is attributed to the use of a different version of the MLS retrieval product from V2 to V3.4, Flemming et al. (2017). The TCR reanalyses underestimate the lower tropospheric ozone after 2011, which could be associated with the lack of TES measurements during the recent years. At higher altitudes (650 and 350 hPa) differences between the reanalyses are relatively smaller. On average at 650 hPa CAMS-iRean shows a slight underestimation (-3.1 ppb), while CAMS-Rean and TCR-1 bias is below 1 ppb, and slightly larger for TCR-2 (2.4 ppb). At 350 hPa all reanalysis products perform overall similar. At this altitude a considerable inter-annual variability is visible in the observations, see Figure S3 in the Supplementary Material, which appears to be well captured by the reanalysis products, with temporal correlations in the order R=0.85 (for TCR-1) to R=0.92 (CAMS-Rean). Also both the observations and reanalyses indicate an upward trend of tropospheric ozone in the Upper Troposphere - Lower Stratosphere (UTLS), as also confirmed by Williams et al., (2019).

Over **Western Europe** the CAMS reanalyses show good correspondence to the observations at 850 hPa from 2004 onwards, with mean biases of -1.9 (CAMS-iRean) and 0.4 ppb (CAMS-Rean). The TCR reanalyses overestimate ozone at lower altitudes, particularly in TCR-1 before 2010, which shows positive biases at 850 hPa of up to ~15 ppb, with an average over the full time period of 3.3 ppb. Such overestimates suggest a strong influence of the forecast model performance for the boundary layer (e.g., mixing and chemistry), while the optimization of the emission precursors was not sufficient to improve the lower tropospheric ozone analysis. At ~650 and ~350 hPa, the reanalyses reproduced well the observed seasonal and interannual variations. As an exception, TCR-1 overestimates ozone for some cases, especially in winter. In contrast, the CAMS reanalyses show average (absolute) biases less than 3.3 ppb at all pressure levels.

Over the **Eastern US**, all the reanalysis products show similar stddev values at ~850 hPa (3.0–4.0 ppb), which is associated with positive analysis biases, mostly during summer by 0.3–6.8 ppb. Such biases have also been reported in dedicated studies (e.g., Travis et al., 2016), which could be associated with model errors, for instance, excessive vertical mixing and net ozone production in the boundary layer. The annual mean bias for the reanalyses ranges between -2.3 and 2.6 ppb. A decrease in the observed ozone concentrations at ~850 hPa after 2014, associated to a change in the number of contributing stations in this evaluation, leads to a general and consistent over-estimate in all of the reanalyses. A similar agreement with the observations was found in the middle troposphere compared to the lower troposphere, with stddev ranging between 2.9 and 4.7 ppb, while at ~350 hPa the stddev ranges between 8.6 and 11.1 ppb.

Over **Japan**, all reanalyses on average overestimate ozone at 850 hPa and 650 hPa before 2011, with relatively large positive biases in TCR-1 and TCR-2 at 650 hPa (7.9 and 6.9 ppb, respectively, when averaged for the 2005-2010 time period). From

2011 onwards the correspondence with observations improves remarkably. The changes in performance statistics for all reanalyses likely have multiple causes. This includes trends in the observed ozone (Verstraeten et al., 2015), associated to changes in Chinese precursor NO_x emissions (e.g. van der A et al., 2017). Also changes in the observing system are important to consider, particularly the reduction of assimilated TES measurements in TCR from 2010 onwards, and the row anomaly issues affecting assimilated OMI O_3 and NO_2, see also Sec. 2.5.

In the **tropics**, all reanalyses except CAMS-iRean overestimate ozone at 850 hPa before 2012, with positive biases in the range 2.5-3 ppb. The different performance for CAMS-iRean from 2012 onwards is probably associated to the use of another version of the MLS retrieval product. Interestingly, both CAMS reanalyses show a strong peak in ozone at 850 hPa during the second half of 2015 (see corresponding Figure S3 in the Supplementary material), but with a zonally averaged overestimation of up to 20 ppb. This is associated to the strong El Niño conditions, and this particular spike was attributed to an over-estimate of ozone observed at the Kuala Lumpur station for October 2015. Here exactly the grid box affected by the extreme fire emissions in Indonesia for this period (Huijnen et al., 2016), as prescribed by the daily GFAS product, has been sampled. This peak appears much weaker in TCR. Possible explanations are lower optimized NO_x and CO emissions in TCR compared to those used in CAMS, resulting in weaker ozone production, together with a coarser reanalysis model resolution.

At 650 hPa, the TCR reanalyses overestimate ozone almost throughout the reanalysis period (by 3.1–3.8 ppb on average), whereas the CAMS-Rean shows closer agreement with the observations (mean bias = 0.5 ppb, stddev = 3.2 ppb). At ~350 hPa, the TCR-2 shows improved agreement compared with the earlier TCR-1, as confirmed by improved mean bias (from 4.3 to 0.6 ppb) although similar stddev (from 4.9 to 4.7 ppb). Also the temporal correlation remains relatively low.

Over the **SH mid-latitudes** an overall good correspondence is obtained for all reanalyses, but particularly CAMS-Rean and TCR-2, throughout the troposphere. This is marked by the lowest magnitudes for stddev and highest for the temporal correlations, for any of the three altitude ranges compared to the statistics in other regions. Nevertheless, CAMS-iRean still underestimates ozone before 2012 in the lower and middle troposphere, whereas TCR-1 overestimates it particularly at 382 hPa after 2010. Furthermore, CAMS-iRean and CAMS-Rean suffer from relatively large negative biases before 2005, particularly at 382 hPa. This is attributed to similar causes as have been discussed for the Arctic region.

A large diversity among the system performance is seen over the **Antarctic**. As in the Arctic region, free tropospheric O_3 in the CAMS reanalyses is comparatively poorly constrained during 2003, as consequence of the use of the NRT data product from MIPAS and early SCIAMACHY data in the assimilation. Also in the period between the end of March and the beginning of August 2004 no profile data were available for assimilation, leading to a temporary degradation in the reanalysis performance.
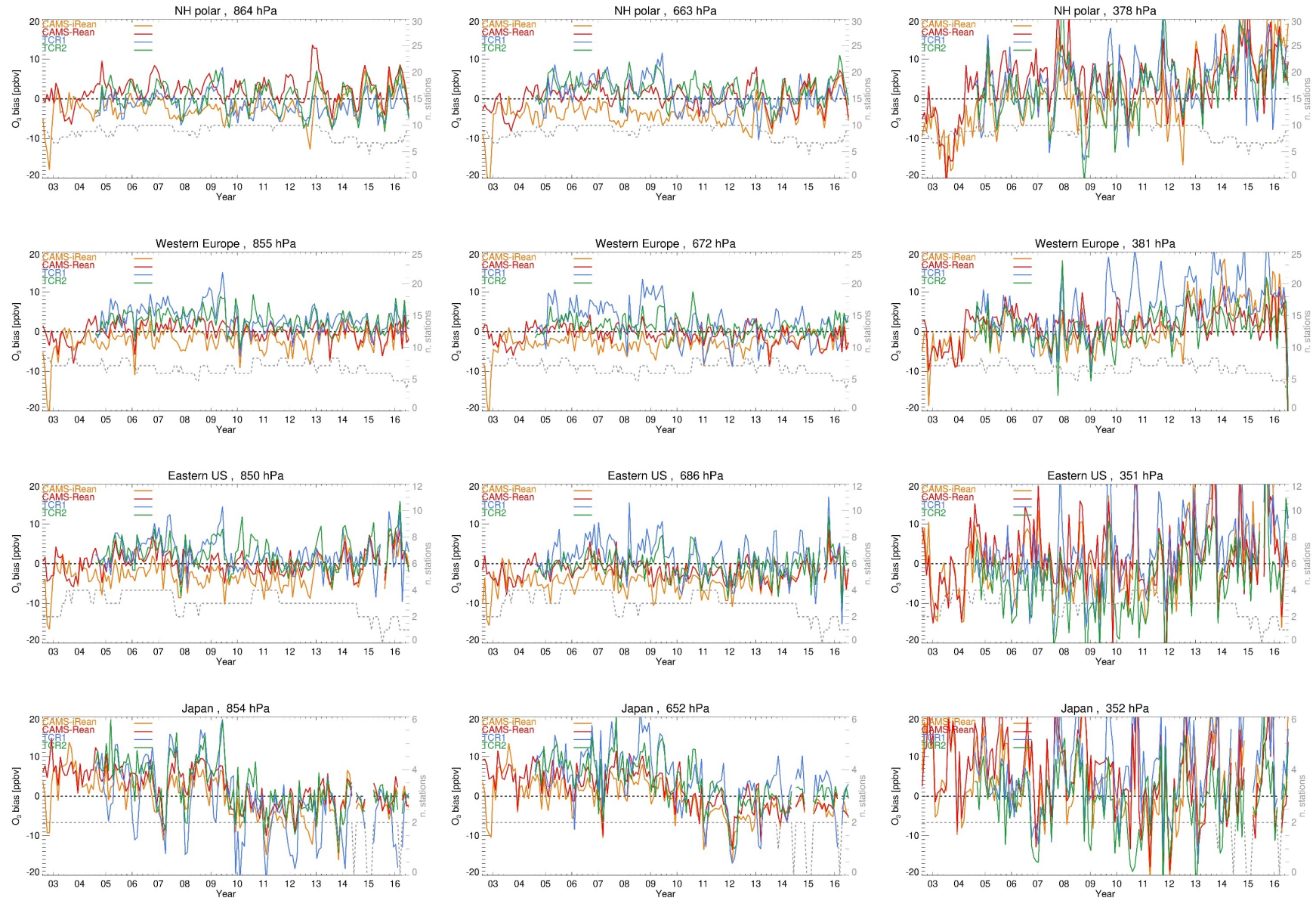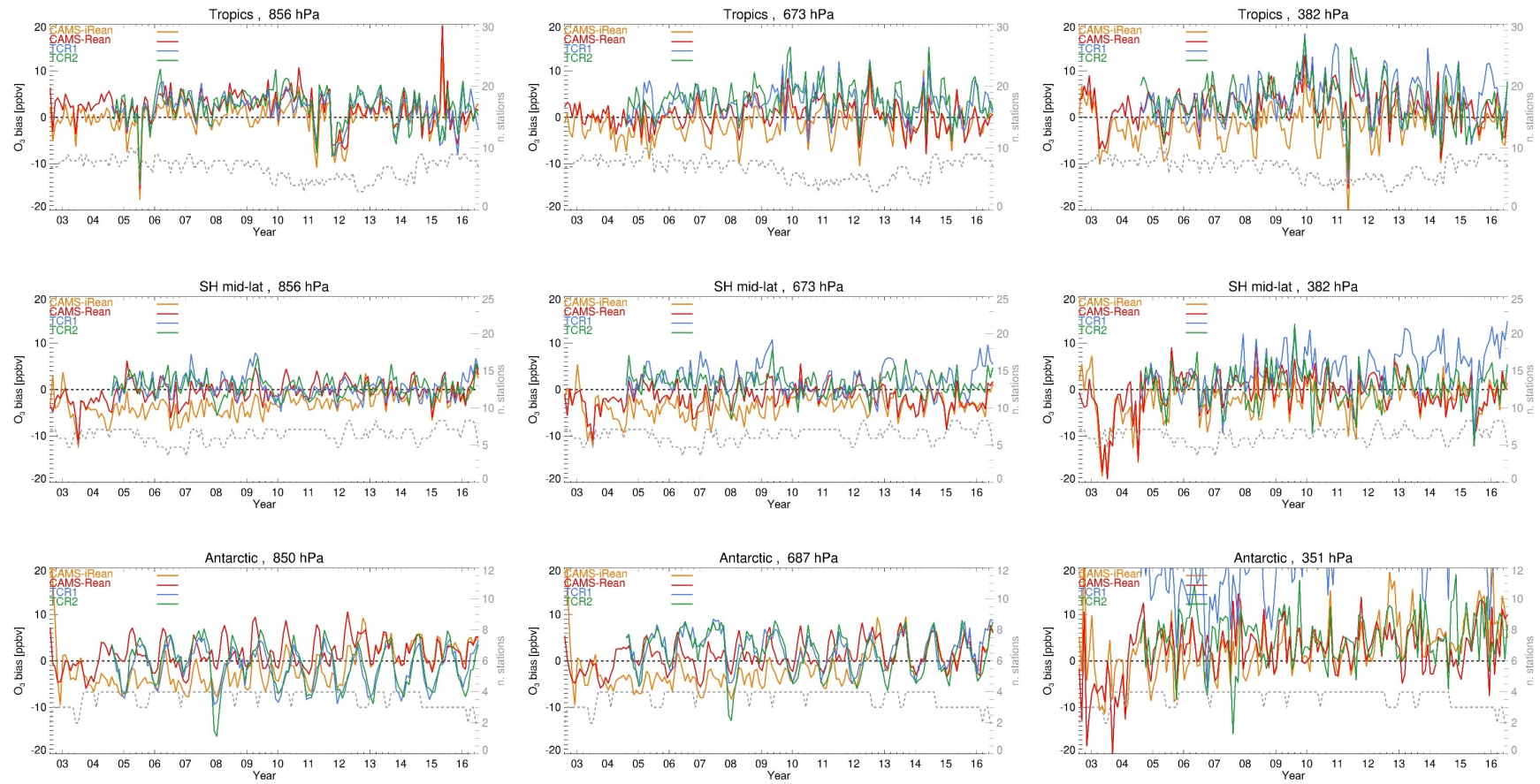
510

Figure 6. Time series of regionally and monthly aggregated ozone biases at different altitudes (850, 650 and 350 hPa), sampled at ozone sonde locations. As in Figure 4, the gray dashed line refers to the number of stations that contribute to the statistics (right vertical axis).

515

520

Before 2013, CAMS-iRean underestimates the low ozone values in the lower and middle troposphere during austral spring, while CAMS-Rean overestimates it during austral winter. Afterwards, both systems show very similar results, also in overall better agreement with the observations, even though an overestimate during austral spring remains. Reasons for the change in behaviour in CAMS-iRean is the change MLS version from V2 to V3.4 after 2012. Furthermore both CAMS-iRean and CAMS-Rean are affected by a change from 6L SBUV to 21L NRT data in January and July 2013 respectively, which appears to contribute significantly to the changes in the bias. The seasonal cycle in the biases can largely be attributed to the lack of O_3 total column observations during polar night, combined with a seasonal variation in model forecast biases. The TCR reanalyses largely underestimate ozone during austral summer and autumn in the lower troposphere. At 351 hPa, TCR-1 substantially overestimates ozone throughout the year (22 ppb on average) because of large model biases and the lack of observational constraints. This large positive bias was resolved in TCR-2 by improving the modelling framework.

In conclusion, evaluation of the tropospheric ozone reanalyses against ozone sondes has revealed the following:

- The updated reanalyses show on average improved performance compared to the predecessor versions, but with some notable exceptions, such as an increased positive bias over the Antarctic in CAMS-Rean versus CAMS-iRean. Over the Antarctic the TCR-2 strongly improved upon TCR-1, despite the lack of direct observational constraints.

- For individual regions or conditions CAMS Reanalysis and TCR-2 show different performance, but averaged for all regions of similar quality. Best performance, in terms of mean bias, standard deviation and correlation, for the updated reanalyses is obtained for the Western Europe, Eastern US and SH mid latitude regions (both normalized mean bias and standard deviation below 8% at 850 and 650 hPa). Relatively worst performance is found for the Antarctic region, with normalized standard deviation up to 18%. This is likely associated to the fewer observational constraints in the polar regions compared to the other regions.

- In terms of temporal consistency, the CAMS Reanalyses show degraded performance over the polar regions during 2003 and 2004, due to lower quality MIPAS and SCIAMACHY data usage. CAMS-iRean also shows a change in performance statistics in the polar regions from 2014 onwards, associated to a changes in the MLS retrieval product versions. Furthermore, both CAMS-Rean and CAMS-iRean are affected by the change in the SBUV/2 product versions in 2013.

With the reduced data-availability from TES from 2010 onwards the TCR tropospheric ozone products show changes in their performances. Remarkably, TCR-1 and TCR-2 show overall slight improvements from 2010 onwards. This is marked by reduced positive biases in the lower troposphere over NH-mid-latitude regions and may be attributed to biases in the TES retrieval product, combined with changes in the OMI product, see also Sec. 2.5. Additional Observing System Experiments (OSEs) are needed to identify the relative roles of individual assimilated measurements on the changes in reanalysis bias.

5. Validation against TOAR surface observations

We evaluated the reanalyses against monthly mean, gridded surface observations filtered for measurements performed at rural sites, as compiled in the TOAR project (Schultz et al., 2017). These evaluations reveal the ability of the reanalysis products to reproduce near-surface background ozone concentrations in terms of mean value and variability, both temporally, on seasonal to annual time scale, and spatially, for various regions over the globe.

5.1 Multiannual mean

Figure 7 shows a map with multiannual mean ozone observations from the TOAR database, for the 2005–2012 time period, as well as the corresponding normalized biases in surface ozone for the reanalysis products. Detailed maps for North America, Europe and East Asia are given in Figure S4 in the Supplementary Material, while the corresponding regional mean biases are given in Table 9.

The TCR-reanalyses show significant positive biases for many regions, with multiannual mean biases of 11.0 ppb and 6.8 ppb over the Eastern and Western US, and 6.7 ppb over Europe in TCR-2. These biases can mainly be attributed to model errors. Mean biases in the CAMS-reanalyses are generally smaller (1.5 ppb and -0.2 ppb for Eastern and Western US, respectively, -1.8 ppb for Europe), but still show substantial spatial variations, as quantified by the root-mean-square of the multiannual mean differences across the various regions, which is 8.9 ppb and 6.1 ppb for Eastern and Western US, and 5.6 ppb over Europe for the CAMS Reanalysis (18, 11 and 11 ppb for TCR-2 for these regions). The mean bias is negative over the Arctic, Europe and the Western US and positive over East Asia and Southeast Asia in both versions of the CAMS reanalyses. The positive regional mean biases over the major polluted regions are reduced by 35 to 55% in TCR-2 as compared with TCR-1. Likewise, the negative biases over the Arctic, Europe, the Western US, and SH mid and high latitudes are reduced by more than 25% in CAMS-Rean as compared with CAMS-iRean, illustrating overall improvements for the newer reanalyses.
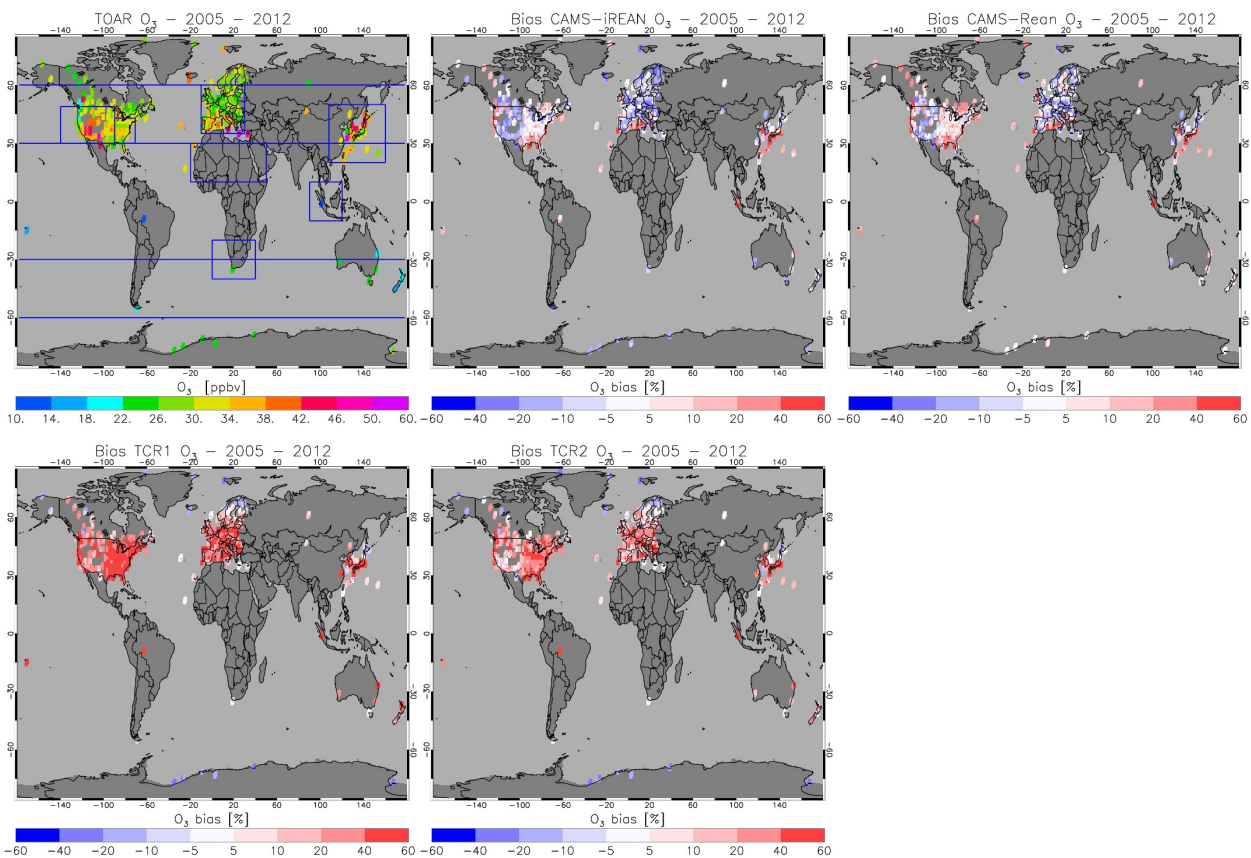
Figure 7: Multiannual (2005-2012) mean surface ozone from TOAR (upper left), along with corresponding normalized mean bias with respect to the observations for the reanalyses.

Table 9. Mean bias (ppb) for the reanalyses against TOAR monthly mean, regional mean observations for the 2005-2012 time period, as sampled for observations in the specified regions indicated in Figure 7.

	Arctic	Europe	Eastern US	Western US	Southeast Asia	East Asia	SH mid-latitudes	Antarctica
CAMS-iRean	-4.5	-2.4	0.1	-1.9	5.6	4.5	-2.2	-3.5
CAMS-Rean	-1.5	-1.8	1.5	-0.2	6.7	2.7	-0.1	1.1

| TCR-1 | -1.8 | 11.2 | 17.2 | 12.9 | 15.8 | 10.5 | 3.6 | -5.7 |
| TCR-2 | -2.3 | 6.7 | 11.0 | 6.8 | 7.4 | 7.6 | 1.5 | -5.4 |

5.2 Variability in regionally averaged surface ozone

Figure 8 presents scatter plots of monthly mean ozone (2005-2012) from the reanalyses against those from the TOAR surface observations for various regions. The corresponding time series, given in Figure S5 in the Supplementary Material, indicate that the main driver of the variation in magnitude of ozone concentrations in the reanalyses and observations is associated to the seasonal cycle. Over the Arctic, the general pattern in the monthly variations is captured for all reanalyses (R between 0.58 and 0.72), although they all underestimate the increased ozone values during boreal spring.

Over Europe and the US, the CAMS reanalyses show the closest agreement with the observations (MB between -2.4 and 1.5 ppb, R>0.8). CAMS-Rean shows improved negative biases for observed low ozone values compared with the CAMS-iRean, which is in boreal winter and spring. The TCR reanalyses exhibit large positive biases over Europe and the US regions (MB between 6.7 and 17 ppb), with significant improvements in TCR-2. Over East Asia, all the reanalyses show positive biases in the range of 2.7 ppb (CAMS-Rean) to 10.5 ppb (TCR-1) and fail to reproduce the minimum concentrations in autumn. Still the temporal correlations are similar to most other regions (R between 0.79 and 0.83), associated with the stable seasonal cycle in both the reanalyses and observations. Over Southeast Asia, positive biases exist throughout the period, which are largest in TCR-1. For this region the TCR-reanalyses show lower temporal correlations (R between 0.39 and 0.49) compared to the CAMS reanalyses (R=0.68).

Significant changes in the surface ozone biases are found in the TCR reanalyses over the SH mid latitudes, with reduced positive biases after 2010. The CAMS reanalyses capture well the temporal variability over the SH mid latitudes and Antarctic (R between 0.89 and 0.96), while CAMS-Rean shows a positive bias for observed high ozone values. This is associated to model biases austral winter (JJA), particularly during 2005-2013, Figure S5. The TCR reanalyses show a significant negative bias throughout the year except for observed low ozone values (during Austral summer) which results in lower temporal correlations (R~0.68).

The free tropospheric intercomparison at different altitudes, as presented in Figure 3, already indicated generally larger biases at 850 hPa compared to 650 hPa. This can be understood as near-surface ozone concentrations are less well constrained by the satellite data products used in the assimilation, and they depend strongly on local conditions such as precursor emissions, deposition, vertical mixing, and chemistry, which are difficult to parameterise at the model grid scale (Sekiya et al., 2018).

An important example of a driver for local variability is the emissions from forest fires which in the CAMS reanalyses are provided through daily-varying GFAS emissions. This has been shown to capture to a good degree the carbon monoxide and aerosol from fire plumes, although larger uncertainties exist in the NO_x emissions, e.g. Bennouna et al. (2019).

In summary, CAMS-Rean shows the best ability to capture the regional mean surface ozone and its variability, while particularly TCR-2 (and to lesser extent also TCR-1) shows positive biases and reduced correlations. Particularly good performance is seen over the western US (R=0.95, MB=-0.2), while over east, and particularly southeast, Asia the performance is poorest.
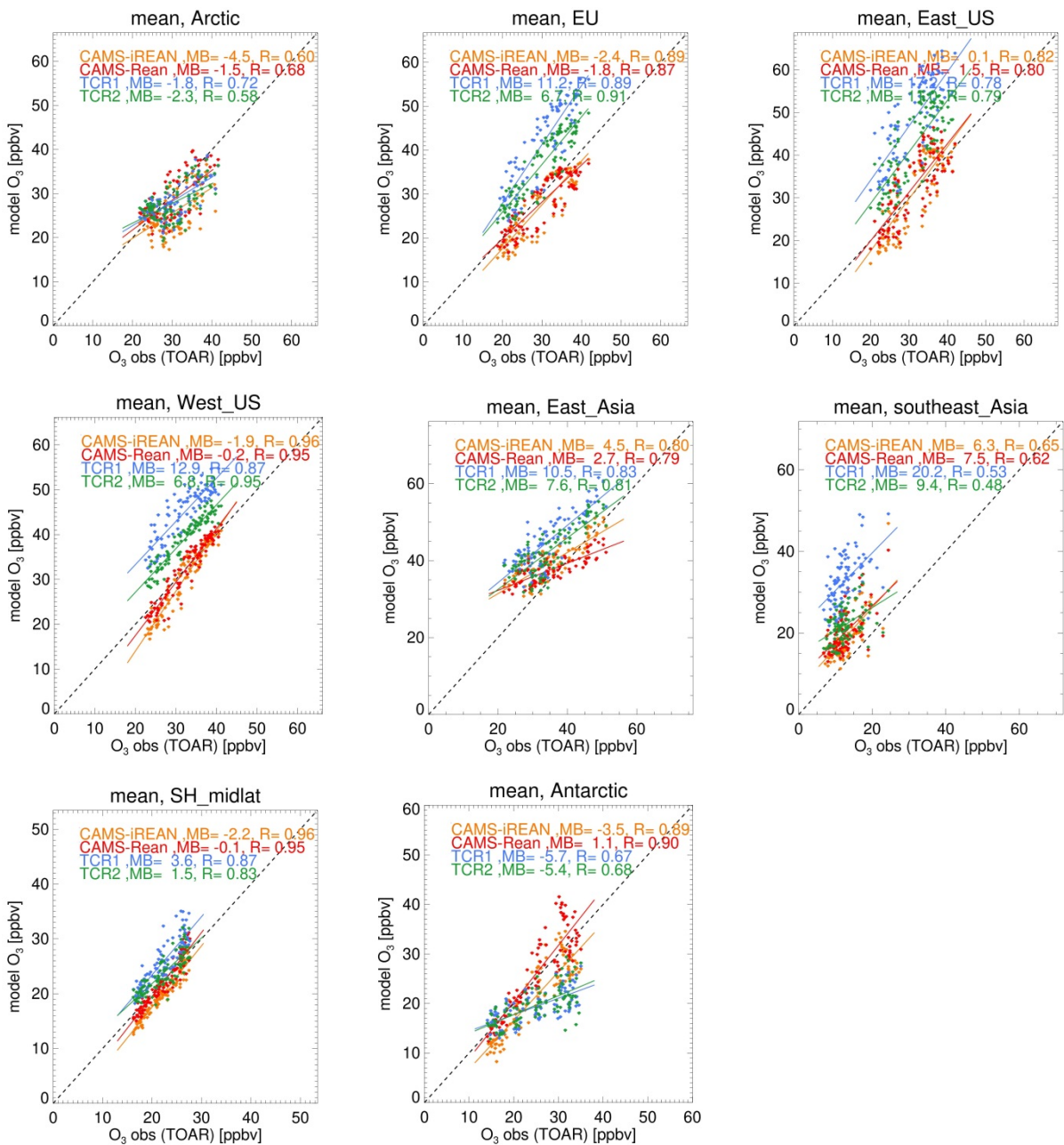
Figure 8: scatter plot of surface ozone against TOAR observations for the 2005-2012 regionally averaged, monthly mean time series. Also the mean bias and temporal correlation is given.

5.3 Interannual variability of regionally averaged surface ozone

We assess the interannual variability (IAV) by computing the deseasonalized anomaly of surface ozone concentrations. For this, the 2005-2012 multiannual monthly, regional mean surface ozone is subtracted from its corresponding instantaneous monthly, regional mean value, both for the reanalyses and for the TOAR observations, see Figure 9. By doing so, we remove the analysis bias, as well as the seasonal cycle. No clear long-term trends are visible in the regional mean surface ozone concentrations. Nevertheless, the observations reveal distinct deviations from the 8-year mean value, which point at temporary anomalies in meteorological conditions and/or emissions. Note that large fluctuations in the time series can also occur due to changes in the observation network. Therefore, when evaluating the temporal correlations between observed and analyzed anomalies we exclude individual months with low data coverage, defined as months where the number of grid boxes with observations is less than half of its average number for the complete time series.

Overall, the reanalysis anomalies are in reasonable general agreement with those seen in the observations, with better skill for regions at low latitudes compared to those at high latitudes. Also for 2003–2004 the CAMS reanalyses mostly show larger deviations than justified from the observations, particularly the first months for CAMS-iRean. This is attributed to the inconsistencies in the assimilated satellite retrieval products as already described. Also the observed positive anomaly associated to the 2003 heatwave period over Europe is therefore not equally seen from the CAMS reanalyses, but with an offset (see also Bennouna et al., 2019). For later years, the magnitude of the anomalies correspond better to the observations. Over the Arctic the temporal correlation is generally low (R<0.33). For Europe CAMS-Rean shows a largest correlation (R=0.49). For the Eastern US region all reanalyses follow an extended dip during 2009, as seen from the observations, and also a second dip during 2013, particularly captured by TCR-2, also resulting in relatively good temporal correlations (R between 0.4 and 0.64). Also, in the Western US the temporal correlations are acceptable (R between 0.42 and 0.56). Over East Asia the correlations are relatively high (R between 0.56 and 0.75), and likewise for the station in Indonesia (southeast Asia) with R=0.45 – 0.63. Here all reanalyses capture the increases in surface ozone in early 2005 and late 2006, and the decrease in 2010.

Over the SH mid latitudes and Antarctic the ozone reanalyses show overall a relatively poor temporal correlation (R<0.37), particularly for TCR (R<0.23). For these regions the TCR reanalyses show larger anomalies during 2007-2009 as compared with observations, whereas the CAMS reanalyses show larger anomalies from 2012 onwards. Figure 9 suggests that this is particularly caused by the change in system behaviour after 2012, as already described in Sec 5.2 evaluating the tropospheric ozone over the Antarctic. As was the case there, for surface ozone the CAMS reanalyses in fact show a better match to the observations from 2013 onwards.

In conclusion, the reanalyses considered here show some skill to capture IAV in monthly mean ozone surface concentrations, in particular for the tropical, sub-tropical and NH mid-latitude regions. In these regions the signal of the observed ozone variability is also larger than for the comparatively stable Arctic conditions. Here the performance is hampered due to changes in the overall bias of the analyses over time.
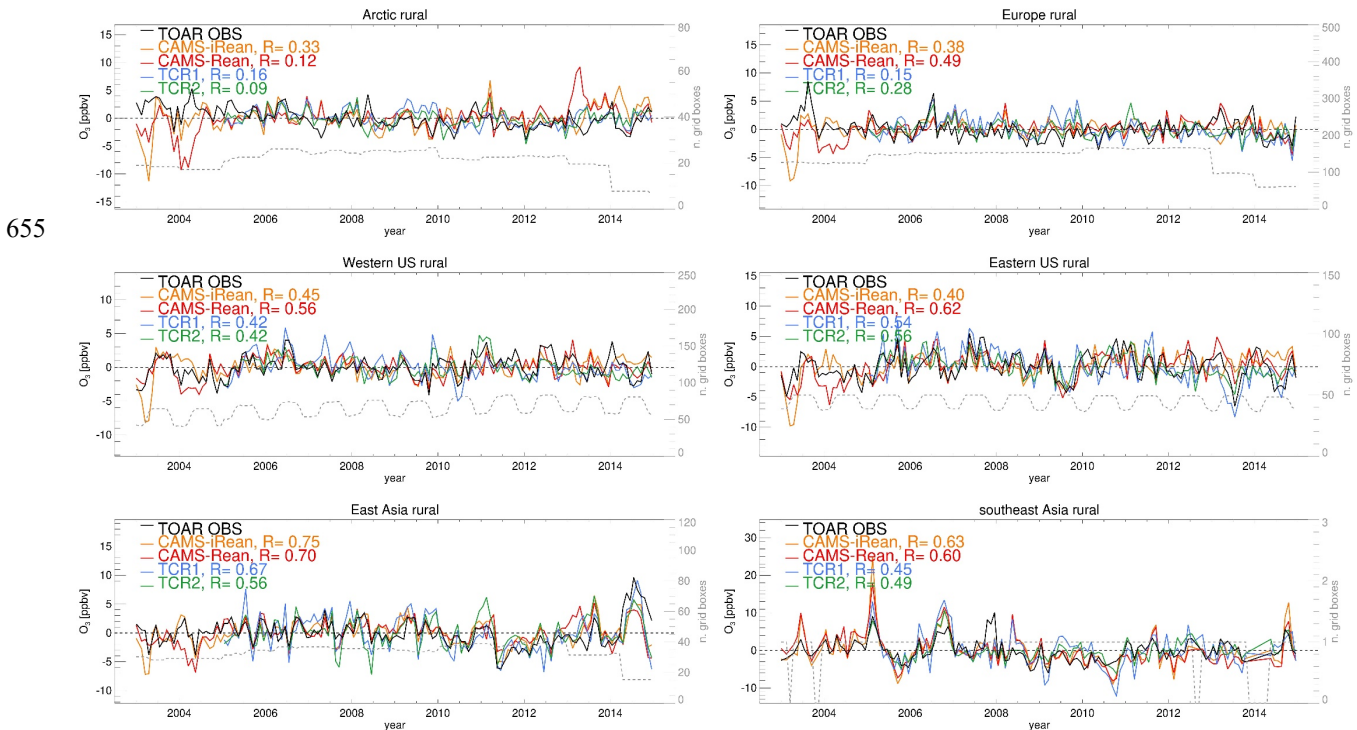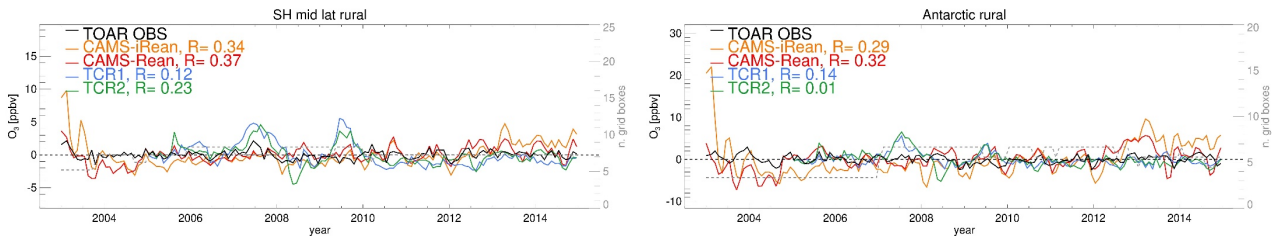
Figure 9: Time series of regional, monthly mean ozone anomalies against those derived from the TOAR observations. The dashed line indicates the number of TOAR 2°×2° grid boxes that contribute to the statistics. Also the temporal correlation as computed for the 2005-2014 time series is given.

6. Evaluation of surface ozone in 2006

To assess the ability of reanalyses to cope with local situations, and specific meteorological conditions, we analysed their performance over Europe in 2006, with a focus on the ability to capture the diurnal and synoptic variability during the heat wave event that affected large parts of Europe during July 2006 (Struzewska and Kaminski, 2008). Here we use the ground-based observations from the EMEP network. For this evaluation we note that these large-scale models do not represent local orography. Therefore we select the appropriate model level depending on its pressure level, which is representative for mean pressure at the observation site (Flemming et al., 2009). Figure 10 presents the evaluation at two EMEP stations in Great Britain, during July 2006, illustrating the general performance of the reanalyses for this situation. The Lullington Heath station (50.8° N, 0.2° E, 120 m.a.s.l.) is located in a Nature Reserve area, near the coast south of London. Great Dun Fell observatory (54.7° N, 2.4° W, 847 m.a.s.l) is located on a mountain summit, approximately 15 km north of Manchester. Both stations show enhanced levels of ozone in the first part of July, as well as during 16-20 July. In contrast to Great Dun Fell, Lullington Heath shows a pronounced diurnal cycle. For this evaluation, the reanalyses are sampled at different model levels (see figure caption). Note that the TCR reanalyses have fewer model levels towards the surface than the CAMS reanalyses. All reanalyses capture both the diurnal and synoptic variability with a significant improvement in TCR-2 compare to TCR-1, while the CAMS reanalyses are more alike. Particularly for Lullington Heath, the CAMS reanalyses and TCR-2 show remarkably small biases (MB < 3.6 ppb). Also at Great Dun Fell the synoptic variability is generally well captured, particularly for the CAMS reanalyses and TCR-2.
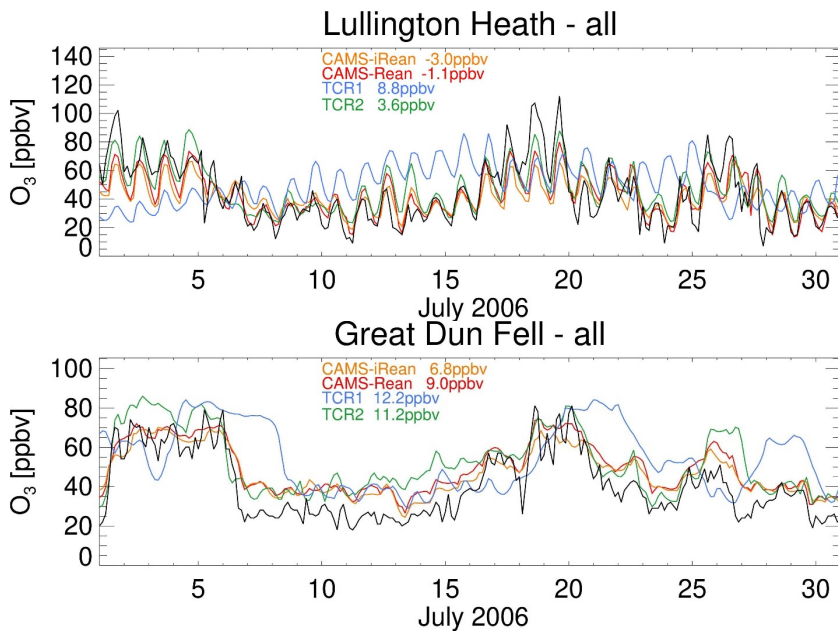
Figure 10: Time series of reanalyses against ozone observations at two EMEP stations in Great Britain during July 2006: Lullington Heath (top, 120m a.s.l., model level 3 (CAMS) and 1 (TCR)) and Great Dun Fell (bottom, 847m a.s.l., model level 8 (CAMS) and 3 (TCR)). Also given are mean biases.

685 A more quantitative assessment of the ability of the reanalyses to capture the ozone variability is presented in Figures 11 and 12, which show a graphical presentation of the temporal correlation coefficient at EMEP stations for December-January-February (DJF) and June-August (JJA) 2006, computed interpolating the reanalyses and observational results onto a common 3-hourly time frequency.

In the DJF period, regionally averaged correlation coefficients range from 0.45 (TCR-1) to 0.58 (CAMS-iRean).
690 Comparatively high correlations were found over western Europe (particularly over the southern part of Britain), with R>0.8 for the CAMS reanalyses, and R>0.6 for TCR. The lower correlations over the regions in the TCR reanalyses could be associated with its coarser model resolution.

For the summer period (JJA, Figure 12), temporal correlations are overall higher than in the winter period, most markedly by better correlation statistics over south-western, eastern and northern Europe. This is due to the more pronounced diurnal
695 cycle during summer and results in generally consistent correlation over any of the stations across the European domain. The average values range between R=0.61 (TCR-1) and 0.68 (CAMS-iRean). Only stations sampling ozone around the Mediterranean are consistently poorly captured, with R<0.5.

Temporal correlations for the March-April-May (MAM) and September-October-November (SON) seasons are in-between those for DJF and JJA. The CAMS-Rean correlations are on average lower by ~0.02 than those of CAMS-iRean, while
700 TCR–2 has systematically improved by 0.02–0.05 over TCR-1.
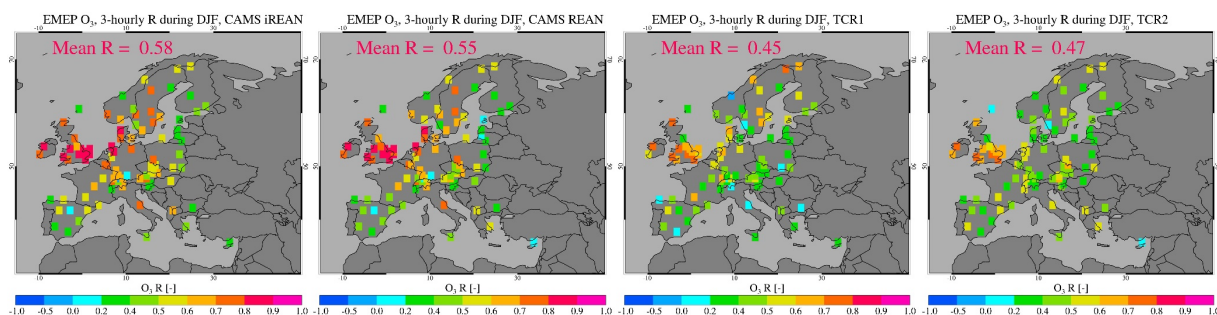
Figure 11: Correlation coefficients computed for 3-hourly DJF 2006 at EMEP stations for the four reanalyses. The mean value, based on correlations computed for all individual stations, is given.
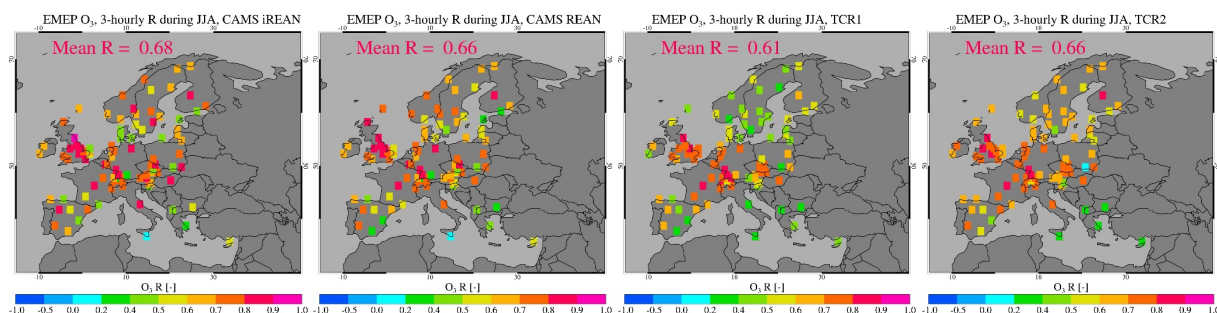
705 **Figure 12: As figure 11, but for JJA.**

A closer look at the diurnal cycle for different seasons and regions over Europe is given in Figure 13. In this figure the seasonal mean reanalysis biases have been subtracted in order to assess their ability to capture the diurnal cycle only. All reanalyses generally capture the diurnal variability, and its variation across latitude region and season. For instance, all
710 reanalyses show little diurnal variability for Northern European stations during DJF, although the CAMS-based reanalyses (and particularly CAMS-Rean) show enhanced night-time O_3, which is not in TCR nor in the observations. Except for isoprene, no diurnal cycle in O_3 precursor emissions has been adopted in the CAMS reanalyses, which contributes to biases in the diurnal cycle. Note, however, that CAMS-Rean shows a comparatively large mean bias for these conditions, of -8 ppb (CAMS-iRean bias is -6 ppb).

715 The diurnal cycle is generally larger for CAMS-iRean than CAMS-Rean, overall showing better correspondence to the observations. Particularly over middle and southern Europe during DJF the CAMS reanalyses show a larger diurnal cycle than those obtained with TCR, also better matching to the observations. For MAM differences between the reanalyses are rather small, while during JJA the TCR-2 and CAMS-iRean show largest diurnal cycle across Europe, best matching again to the observations.

720 In summary, all reanalyses capture the synoptic to diurnal variability, as illustrated by the assessment of the heatwave event in July 2006. Still there are considerable differences in performance, depending on the reanalysis, region and season. While CAMS-iRean and CAMS-Rean perform mostly similar, for TCR-2 a considerable improvement was found compared to TCR-1. Overall better temporal correlations are obtained for the summer period compared to winter, and also for Western Europe compared to the Mediterranean region. Further improvements can be obtained by a better description of surface

725 processes, including emissions and deposition, together with higher spatial resolution modelling.
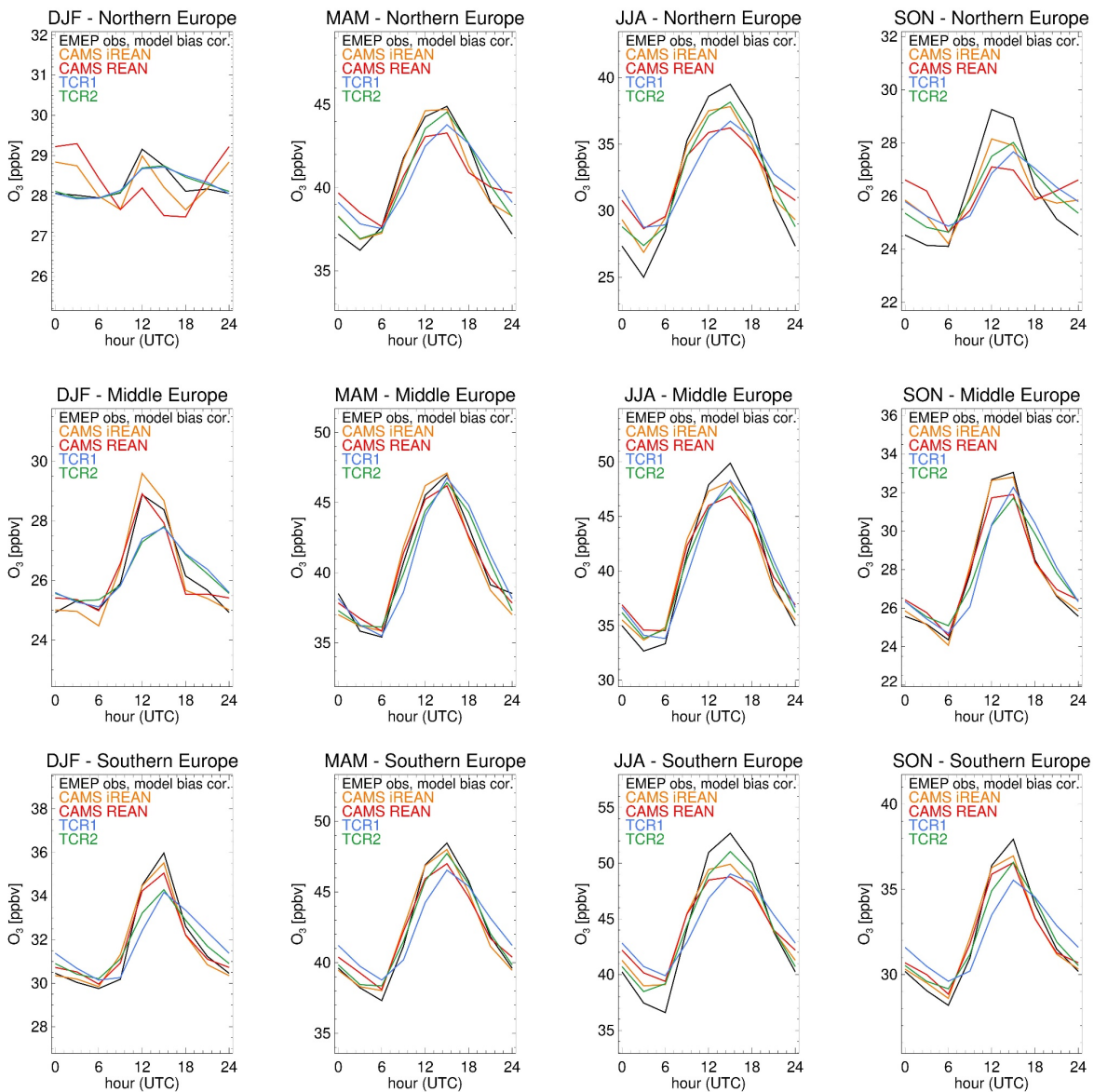
730 **Figure 13: Plots of seasonal mean diurnal cycle against EMEP observations for 2006. Middle-Europe is here defined as the region between 35°N and 45°N, with Northern (Southern) Europe at higher (lower) latitudes. Note that the reanalysis bias has been removed. Model level selection is through matching of the reanalysis pressure with pressure level of the station sites.**

7. Global spatial and temporal consistency between reanalyses

Figure 14 shows the multiannual mean together with an evaluation of its multi-system standard deviation, at different altitude levels. The standard deviation is computed from the multiannual means of the four reanalyses, and provides a quantification of general agreement between reanalyses. The standard deviation at 850 and 650 hPa is relatively large over South America, Central Africa and Northern Australia, with values exceeding 6 ppb in the lower and middle troposphere. Normalized to local mean O_3 from the CAMS Reanalysis, the standard deviation values at 850 hPa reach 20% over Australia and up to 50% over South America and Central Africa. At 650 hPa these maximum ratios decrease to approx. 10% (Australia) and 20% (South America and Central Africa). These results suggest that the representation of biomass burning emissions and its impacts on ozone production are largely different among the systems. Also large uncertainties in biogenic emissions likely contribute. In TCR, the optimization of NO_x emissions can have strong impacts on the lower and middle tropospheric ozone, in contrast to the CAMS configuration which applies prescribed anthropogenic and biogenic emissions, combined with the daily varying biomass burning emissions. In addition, different representations of convective transport over the continents can lead to diversity in the vertical profile of ozone among the systems.

At 350 hPa, the multi-system standard deviation is large over Central Africa, South America and over the Arctic and Antarctic, which could reflect different representations of deep convection along with biomass burning emissions at low latitudes, and polar vortex, stratospheric ozone intrusions and chemistry treatment at high latitudes among the systems.

The absolute differences between the two most recent reanalyses, TCR-2 and CAMS-Rean, are also shown. Apart from the regions mentioned above, differences are significant around Alaska and Siberia, regions with tropospheric ozone influenced by biomass burning events and where observational constraints at such high latitudes are more limited. Such larger discrepancies once again highlight the importance of the forecast model performance in the reanalysis system as discussed in Miyazaki et al. (2019b), especially when direct observational constraints on tropospheric ozone are insufficient.

An evaluation of the consistency across the four reanalyses to describe the seasonal cycle of tropospheric ozone columns, and its interannual variability, is given in the Supplementary Material, Figure S6. From this, the difference in zonal mean partial columns (surface – 300hPa) in the tropics is quantified: TCR-2 is on average higher than CAMS-Rean by 0.7 DU (2005) up to 1.8 DU (2016), corresponding to approx. 3 to 8% of the annual mean column in this region.

Frequency distributions of the multiannual mean ozone concentrations in the four reanalyses at three altitude levels are given in Figure 15 and summarize the general differences discussed above. In the lower and mid-troposphere the CAMS reanalyses show a larger frequency of O_3 values below 30 ppb (850 hPa) and 45 ppb (650 hPa) compared to particularly TCR-1, but also TCR-2. This is associated to lower ozone in the CAMS reanalyses over the tropical regions. At 350 hPa the CAMS reanalyses and TCR-2 agree reasonably in their frequency distribution, with CAMS-iRean showing the largest frequency of relatively low (35-55 ppb) O_3 values and instead TCR-1 a larger frequency of values in the range 70-100 ppb compared to the other reanalyses. This is associated to a positive reanalysis bias in this altitude range (see also Table 7). A corresponding evaluation of the frequency distributions, but sampled at individual ozone sonde observations during the 2005-2016 period is given in Figure S7 in the Supplementary material. Because of the different sampling approach the shape of the frequency distributions is different than was seen in Figure 15. Evaluation of the sum in absolute differences d between analyzed and observed frequency distributions indicates that at 850 hPa the performance between the four reanalyses is very similar (d between 0.17 and 0.19), while at 650 hPa CAMS-Rean is superior (d=0.13). CAMS-iRean shows an under-estimate of the frequency of high ozone values (larger than ~55 ppbv) at 850 and 650 hPa, explaining the worst performance at 650 hPa (d=0.20). At 350 hPa the differences in performance between reanalyses are largest, with best correspondence to observations for CAMS-iRean (d=0.11), and worst for TCR-1 (d=0.43).

Deseasonalized anomalies in monthly mean ozone tropospheric columns (surface to 300 hPa) have been computed over various regions by subtracting the reanalysis-specific mean seasonal cycle based on the 2005-2016 time series. Figure 16 presents the reanalysis anomalies together with the Multivariate ENSO Index (MEI), (Wolter and Timlin, 1998) for two

regions. Tropical tropospheric ozone variations during El Niño conditions are in part associated with enhanced fire emissions, and corresponding ozone production, over Indonesia, together with suppressed convection (Inness et al., 2015), while the anti-correlation over the eastern Pacific is related to enhanced convection (Ziemke and Chandra, 2003). We find a significant correlation with R ranging between 0.6 (CAMS-Rean) and 0.65 (TCR-2) for the Southeast Asia region. A strong anti-correlation for the eastern Pacific region is found with R between -0.70 (CAMS-Rean) and -0.78 (TCR-2). The CAMS iREAN shows a lower correlation for this region, possibly associated with the jump in offset around the beginning of 2013, whose magnitude is significant in comparison to the signal.

An assessment of the consistency between all reanalyses to describe the deseasonalized anomalies in various regions is given in the Supplementary Material, Figure S8 and Table S1, in terms of the correlations in their anomalies. Specifically, the correlations between CAMS-Rean and TCR-2 over the Arctic, and the Eastern US, are R=0.60 and R=0.63, respectively, giving some confidence in the robustness of this IAV signal in these reanalyses. For various other regions correlations are R=0.52 (Eastern Asia), R=0.42 (Europe) and R=0.33 (Antarctica). Also, when averaged over the full tropical zonal band the correlation decreases to R=0.33, i.e. much smaller than correlations between CAMS-Rean and TCR-2 for the sub-regions Southeast Asia (R=0.82) and ENSO_3.4 (R=0.78). This implies that many of the IAV signals in the reanalyses should be considered with care.
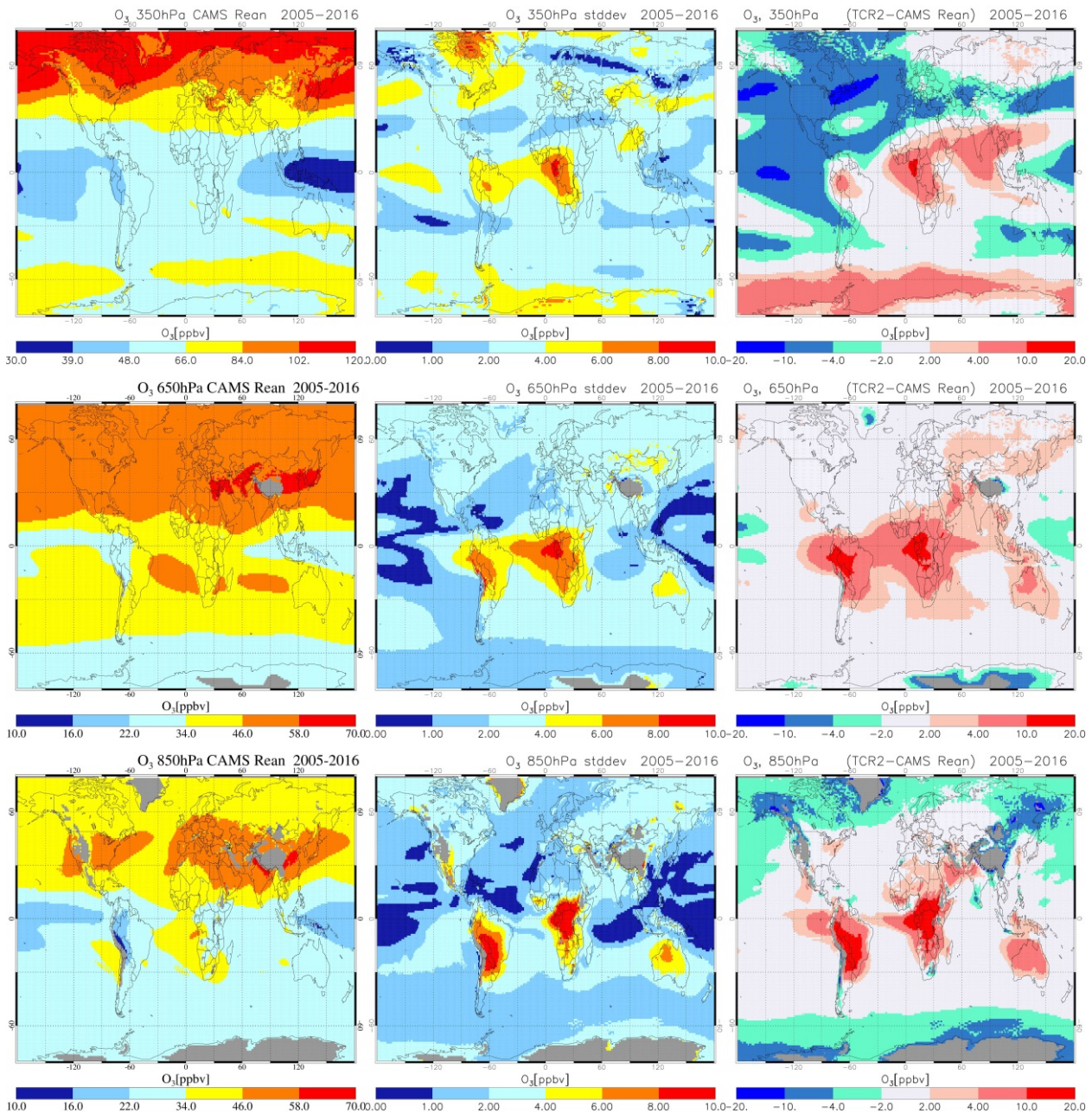
Figure 14: Left: multiannual mean O₃ at 350, 650 and 850 hPa for the CAMS Reanalysis at 650 hPa over 2005-2016. Middle: standard deviation in the multiannual means for the four reanalyses. Right: absolute difference between TCR-2 and CAMS Reanalysis, all in units ppb.

795
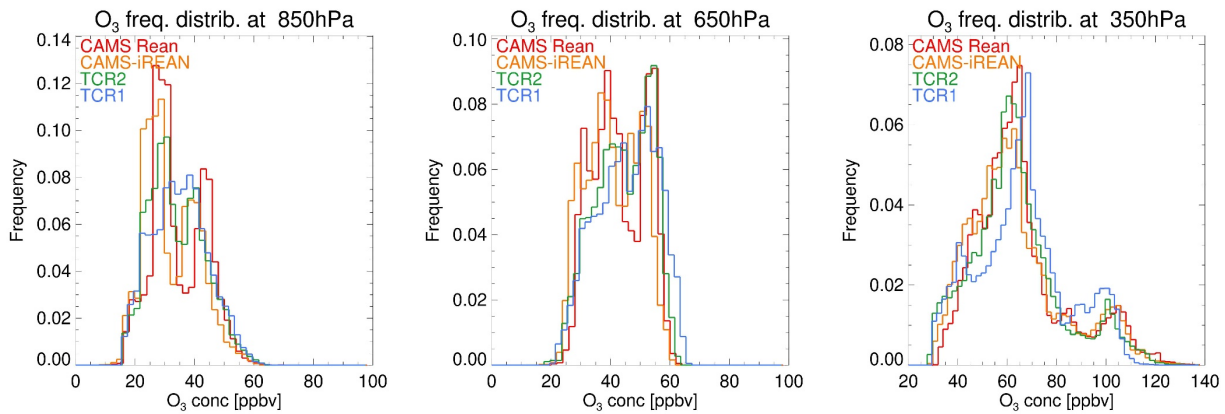
Figure 15: Area-normalized frequency distributions of multiannual (2005-2016) mean O₃ mixing ratios at 850 (left), 650 (middle) and 350 hPa (right) for the four reanalyses.

800
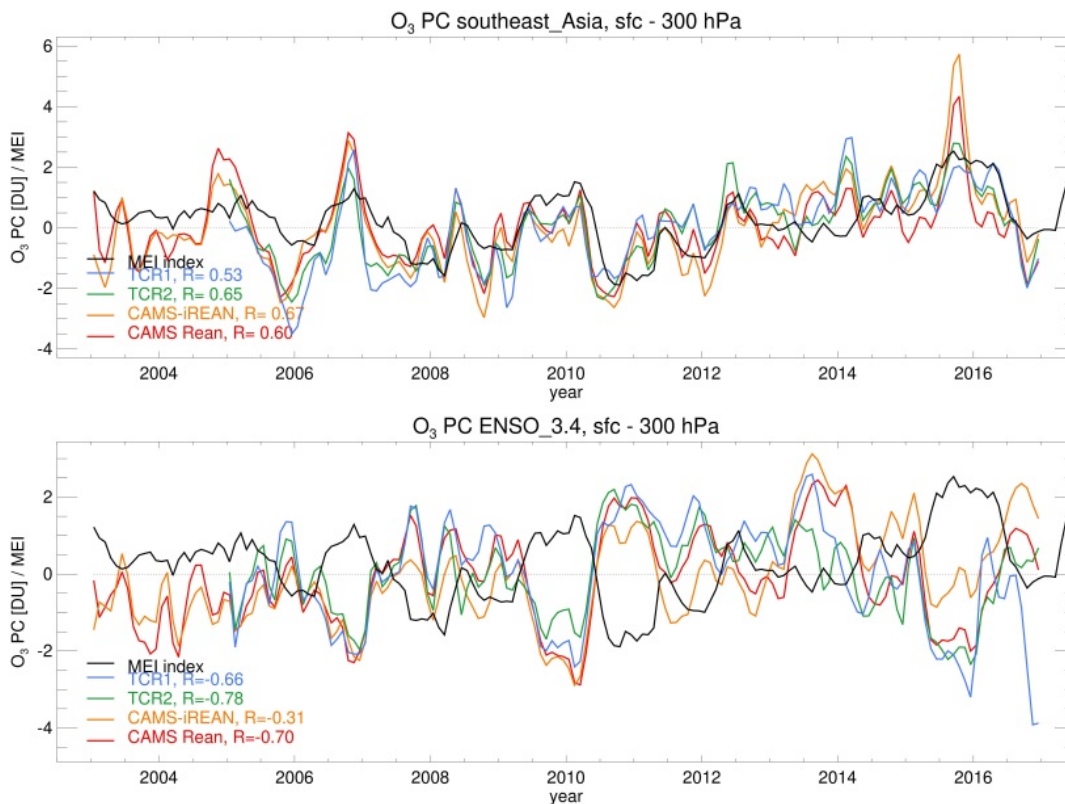
Figure 16: Deseasonalized anomalies in O₃ partial columns (surface to 300 hPa) in four reanalyses, as compared to the MEI index for two regions: Southeast Asia (90° E - 120° E; 10° S - 20° N) and ENSO3.4 over the Eastern Pacific (120W-170W; 5S-5N). A 2-month smoothing has been applied to the reanalysis data, (as for the MEI index). Temporal correlations with respect to the MEI index are given in the legends. Correlations are calculated on monthly data for the 2005-2016 time period.

8. Conclusions and discussion

Four tropospheric ozone reanalyses have been compared in this paper, namely CAMS-iRean, CAMS-Rean, TCR-1, and TCR-2. A range of independent observations was used to validate the quality of the chemical reanalyses at various spatial and temporal scales. These reanalyses aim to capture individual large-scale events, such as heat waves or wildfires, and at the same time aim to provide a globally consistent climatology of present-day composition. This implies stringent requirements on their temporal consistency. The changes in the observing system, combined with often their limited sensitivity to tropospheric profiles and in particular the boundary layer, imply a significant dependency on the global chemistry model, its transport scheme, and its emissions, and makes the generation of any long-term chemical reanalysis challenging. This gives rise for a detailed evaluation of the capability of the current reanalyses of tropospheric ozone, as presented here.

Consistent with Inness et al., (2019), our evaluation also shows substantial improvement of CAMS-Rean over CAMS-iRean in the free troposphere, as quantified by lower mean biases, standard deviations and higher correlations to ozone sonde observations, and better temporal consistency in multiannual time series of tropospheric ozone columns. For instance, averaged over the NH mid latitude region the mean bias in tropospheric ozone columns (surface to 300 hPa) is -0.3 DU (corresponding to approx. 1% of observed tropospheric column) for CAMS-Rean, which was 0.8 DU (3%) in CAMS-iRean. At the surface the CAMS-Rean has generally improved with respect to CAMS-iRean, assessed through evaluations of monthly mean surface concentrations against TOAR observations. Nevertheless, similar performance of both CAMS reanalyses was seen for hourly to sub-seasonal variability assessed with EMEP observations over Europe for the year 2006.

The improved performance in the free troposphere can be attributed to a mixture of various upgrades, including revisions in the chemical data assimilation configuration, the chemistry mechanism, meteorological driver, model resolution, biogenic emissions.

Significant changes in the quality of the ozone reanalyses for different years have been attributed to changes over time in the observing system. Both CAMS reanalyses suffered from the use of relatively poor SCIAMACHY and MIPAS data products before 2005, which improved afterwards. Also across 2013 in CAMS-iRean was affected by a switch of MLS version 2 to version 3.4. In both CAMS reanalyses a change to the vertical resolution of the assimilated SBUV/2 data during 2013 had a negative impact on the consistency of multiannual tropospheric ozone time series, particularly in polar regions. Inness et al. (2019) had noticed such a change in performance, but had not yet identified the responsible observational dataset.

Compared with TCR-1, TCR-2 shows better agreements with independent observations throughout the troposphere, including at the surface. Similar to the CAMS reanalyses, for the NH mid latitudes the mean bias in tropospheric columns against ozone sondes improved from 1.8 DU (7%) in TCR-1 to 0.8 DU (3%) in TCR-2. The improvements can be attributed to the use of more recent satellite retrievals and to an improved model performance, mainly associated with the increased model resolution. In spite of the good agreement with ozonesonde measurements in the free troposphere, the surface ozone reanalysis exhibits large positive biases over Europe and the United States. Also, the lack of the TES measurements led to a change in the reanalysis performance after 2010 for many regions in the lower and middle troposphere. Changes in the NO_2 observing system, including the OMI row anomaly after December 2009 and the limited temporal coverage of SCIAMACHY and GOME-2, are also considered to affect long-term consistency. The data assimilation diagnostics indicate the need for additional observational constraints, possibly combined with stronger inflation of the forecast error covariance, to improve the long-term reanalysis performance and to measure the actual analysis uncertainty.

Whereas free tropospheric ozone reanalyses agree well with independent observations, towards the surface larger biases have been found for many parts over the globe.. A large spread at high latitudes could also be associated with the limited constraints from (tropospheric) ozone measurements. In these conditions the reanalyses depend more on the model performance and their emissions. Recently developed retrievals with high sensitivity to the lower troposphere (e.g. Deeter et al., 2013; Fu et al., 2018; Cuesta et al., 2018) would be helpful in improving the analysis of the lower troposphere. Furthermore, in future studies the analysis ensemble spread from EnKF can be regarded as uncertainty information about the analysis mean fields, indicating the need for additional observational constraints. Likewise, in the 4-D Var system the contributions from individual retrieval products can be tested.

We have demonstrated that the recent chemical reanalyses of CAMS-Rean and TCR-2 agree well with each other and with the independent observations in the majority of cases. This highlights the usefulness of the current chemical reanalyses in a variety of studies. For instance, the well-characterized, small mean bias in tropospheric columns in these reanalyses suggest that they can be used to provide a climatology of present-day tropospheric ozone. This may serve as a reference for the present-day contribution of tropospheric ozone to the radiation budget, or may provide a climatology for a-priori ozone profiles as required for satellite retrieval products (e.g., Fu et al., 2018). The ability of the CAMS Reanalysis to capture the variability of (near-)surface ozone on multiple time scales, and for many regions over the globe, indicates it is fit for use as boundary conditions for hindcasts of regional air quality models.

Meanwhile, our intercomparisons suggest that the model configuration can still explain differences in the ozone reanalyses. For instance, differences in the representation of convective transport over the continents and those in the precursor's emissions, as well as differences in the chemical scheme, lead to substantial differences in the vertical profile of ozone and ozone production, such as over Central Africa and South America. Here the standard deviation in annual mean ozone at 850 hPa reaches up to 50% of the multi-reanalysis mean. The relatively coarse horizontal resolution in any of the global reanalysis configurations could also cause significant errors at urban sites. Therefore both the data assimilation settings and

the model performance are critical in improving the tropospheric ozone analysis and obtaining consistent data assimilation analysis, especially for the lower troposphere.

We have shown that discontinuities in the availability, coverage and product version of the assimilated measurements affect the quality of any of the reanalyses, particularly in terms of temporal consistency. This is particularly important for assessing interannual variability. The influence of data discontinuities must be considered and where possible removed when studying interannual variability and trends using products from these reanalyses. To improve the temporal consistency in future reanalyses, a careful assessment of changes in the assimilation configuration, most prominently associated with ozone column and profile assimilation is needed, including a detailed assessment of biases between various retrieval products.

The assimilation of multi-species data in both the CAMS and TCR configurations influences the representation of the entire chemical system, while the influence of persistent model errors in complex tropospheric chemistry continues to be a concern. Therefore, further improvements to long-term reanalyses of tropospheric ozone can be achieved by improving the observational constraints, together with a further optimization of model parameters, such as the chemical mechanism, emission, deposition, and mixing processes.

Data availability

The CAMS reanalyses data are freely available from https://atmosphere.copernicus.eu/ (last access: 18 October 2019). The TCR-1 reanalysis is available from https://ebcrpa.jamstec.go.jp/~miyazaki/tcr/ , the TCR-2 reanalysis is available from https://tes.jpl.nasa.gov/chemical-reanalysis/.

Author contributions

VH and KM designed the study and wrote large parts of the manuscript. VH performed the evaluations and analyses. JF and AI provided the CAMS-Reanalysis data, KM and TS provided the TCR-Reanalysis data. MGS provided the TOAR data, and contributed to its interpretation. All co-authors contributed to the writing and the analyses.

Acknowledgements

We thank three anonymous reviewers for their critical comments, which have helped to improve the quality of the manuscript. We acknowledge the use of data products from the NASA AURA, EOS Terra, and Aqua satellite missions. Part of the research was carried out at the Jet Propulsion Laboratory, California Institute of Technology, under a contract with the National Aeronautics and Space Administration. We also acknowledge the free use of tropospheric NO_2 column data from the SCIAMACHY, GOME-2, and OMI sensors from http://www.qa4ecv.eu and. This work was supported through JSPS KAKENHI grant number 18H01285 and the Environment Research and Technology Development Fund (2-1803) of the Ministry of the Environment, Japan, and by the Post-K computer project Priority Issue 4 - Advancement of meteorological and global environmental predictions utilizing observational Big Data. The Earth Simulator was used for simulations as "Strategic Project with Special Support" of Japan Agency Marine-Earth Science and Technology. Part of this work was performed at the Jet Propulsion Laboratory, California Institute of Technology, under a contract with the National Aeronautics and Space Administration. The Copernicus Atmosphere Monitoring Service is operated by the European Centre for Medium- Range Weather Forecasts on behalf of the European Commission as part of the Copernicus Programme (http://copernicus.eu, last access: 15 March 2019). We thank all research and agency teams who provided data to WOUDC, SHADOZ, TOAR, and EMEP.

References

Bennouna, Y., M. Schulz, Y. Christophe, H.J. Eskes, S. Basart, A. Benedictow, A.-M. Blechschmidt, S. Chabrillat, H. Clark, E. Cuevas, H. Flentje, K.M. Hansen, U. Im, J. Kapsomenakis, B. Langerock, K. Petersen, A. Richter, N. Sudarchikova, V. Thouret, A. Wagner, Y. Wang, C. Zerefos, Validation report of the CAMS global Reanalysis of aerosols and reactive gases, years 2003-2017, Copernicus Atmosphere Monitoring Service (CAMS) report, CAMS84_2018SC1_D5.1.1-2017_v1.pdf, 2019, doi:10.24380/xjhk-zt69.

Bhartia, P. K., McPeters, R. D., Mateer, C. L., Flynn, L. E., and Wellemeyer, C., Algorithm for the estimation of vertical ozone profiles from the backscattered ultraviolet technique, J. Geophys. Res., 101(D13), 18,793– 18,806, 1996.

Bocquet, M., Elbern, H., Eskes, H., Hirtl, M., Žabkar, R., Carmichael, G. R., Flemming, J., Inness, A., Pagowski, M., Pérez Camaño, J. L., Saide, P. E., San Jose, R., Sofiev, M., Vira, J., Baklanov, A., Carnevale, C., Grell, G., and Seigneur, C.: Data assimilation in atmospheric chemistry models: current status and future prospects for coupled chemistry meteorology models, Atmos. Chem. Phys., 15, 5325-5358, https://doi.org/10.5194/acp-15-5325-2015, 2015.

Boersma, K. F., Eskes, H. J., Dirksen, R. J., van der A, R. J., Veefkind, J. P., Stammes, P., Huijnen, V., Kleipool, Q. L., Sneep, M., Claas, J., Leitão, J., Richter, A., Zhou, Y., and Brunner, D.: An improved tropospheric NO2 column retrieval algorithm for the Ozone Monitoring Instrument, Atmos. Meas. Tech., 4, 1905-1928, https://doi.org/10.5194/amt-4-1905-2011, 2011.

Boersma, K. F., Eskes, H., Richter, A., De Smedt, I., Lorente, A., Beirle, S., Van Geffen, J., Peters, E., Van Roozendael, M. & Wagner, T., QA4ECV NO$_2$ tropospheric and stratospheric vertical column data from OMI (Version 1.1) [Data set]. Royal Netherlands Meteorological Institute (KNMI). http://doi.org/10.21944/qa4ecv-no2-omi-v1.1, 2017a.

Boersma, K. F., Eskes, H., Richter, A., De Smedt, I., Lorente, A., Beirle, S., Van Geffen, J., Peters, E., Van Roozendael, M. & Wagner, T., QA4ECV NO$_2$ tropospheric and stratospheric vertical column data from GOME-2A (Version 1.1) [Data set]. Royal Netherlands Meteorological Institute (KNMI). http://doi.org/10.21944/qa4ecv-no2-gome2a-v1.1, 2017b.

Boersma, K. F., J. van Geffen, H. Eskes, R. van der A, I. De Smedt, M. Van Roozendael, H. Yu, A. Richter, E. Peters, S. Beirle, T. Wagner, A. Lorente, T. Scanlon, S. Compernolle, J.-C. Lambert, Product Specification Document for the QA4ECV NO2 ECV precursor product, Royal Netherlands Meteorological Institute (KNMI), available at http://temis.nl/qa4ecv/no2col/QA4ECV_NO2_PSD_v1.1.compressed.pdf, 2017c

Cariolle, D. and Teyssèdre, H.: A revised linear ozone photochemistry parameterization for use in transport and general circulation models: multi-annual simulations, Atmos. Chem. Phys., 7, 2183–2196, https://doi.org/10.5194/acp-7-2183-2007, 2007.

Checa-Garcia, R., Hegglin, M. I., Kinnison, D., Plummer, D. A., & Shine, K. P. (2018). Historical tropospheric and stratospheric ozone radiative forcing using the CMIP6 database. Geophysical Research Letters, 45, pp 3264-3273. https://doi.org/10.1002/2017GL076770

Cheung, J. C. H., Haigh, J. D., and Jackson, D. R. (2014), Impact of EOS MLS ozone data on medium-extended range ensemble weather forecasts, J. Geophys. Res. Atmos., 119, 9253– 9266, doi:10.1002/2014JD021823.

Cooper, OR, Parrish, DD, Ziemke, J, Balashov, NV, Cupeiro, M, Galbally, IE, Gilge, S, Horowitz, L, Jensen, NR, Lamarque, J-F, Naik, V, Oltmans, SJ, Schwab, J, Shindell, DT, Thompson, AM, Thouret, V, Wang, Y and Zbinden, RM. 2014. Global distribution and trends of tropospheric ozone: An observation-based review. Elementa: Science of the Anthropocene 2. DOI: 10.12952/journal.elementa.000029

Cuesta, J., Kanaya, Y., Takigawa, M., Dufour, G., Eremenko, M., Foret, G., Miyazaki, K., and Beekmann, M.: Transboundary ozone pollution across East Asia: daily evolution and photochemical production analysed by IASI + GOME2 multispectral satellite observations and models, Atmos. Chem. Phys., 18, 9499-9525, https://doi.org/10.5194/acp-18-9499-2018, 2018.

Davis, S. M., Hegglin, M. I., Fujiwara, M., Dragani, R., Harada, Y., Kobayashi, C., Long, C., Manney, G. L., Nash, E. R., Potter, G. L., Tegtmeier, S., Wang, T., Wargan, K., and Wright, J. S.: Assessment of upper tropospheric and stratospheric water vapor and ozone in reanalyses as part of S-RIP, Atmos. Chem. Phys., 17, 12743-12778, https://doi.org/10.5194/acp-17-12743-2017, 2017.

Dee, D. P., Uppala, S. M., Simmons, A. J., Berrisford, P., Poli, P., Kobayashi, S., Andrae, U., Balmaseda, M. A., Balsamo, G., Bauer, P., Bechtold, P., Beljaars, A. C. M., van de Berg, L., Bidlot, J., Bormann, N., Delsol, C., Dragani, R., Fuentes, M., Geer, A. J., Haimberger, L., Healy, S. B., Hersbach, H., Hólm, E. V., Isaksen, L., Kållberg, P., Köhler, M., Matricardi, M., McNally, A. P., Monge-Sanz, B. M., Morcrette, J.-J., Park, B.-K., Peubey, C., de Rosnay, P., Tavolato, C., Thépaut, J.-N. and Vitart, F., The ERA-Interim reanalysis: configuration and performance of the data assimilation system. *Q.J.R. Meteorol. Soc.*, 137: 553–597. doi:10.1002/qj.828, 2011.

Deeter, M. N., Martínez-Alonso, S., Edwards, D. P., Emmons, L. K., Gille, J. C., Worden, H. M., Pittman, J. V., Daube, B. C., and Wofsy, S. C.: Validation of MOPITT Version 5 thermal-infrared, near-infrared, and multispectral carbon monoxide profile retrievals for 2000–2011, *J. Geophys. Res. Atmos.*, 118, 6710– 6725, doi:10.1002/jgrd.50272, 2013

Deeter, M. N., Edwards, D. P., Francis, G. L., Gille, J. C., Martínez-Alonso, S., Worden, H. M., and Sweeney, C.: A climate-scale satellite record for carbon monoxide: the MOPITT Version 7 product, Atmos. Meas. Tech., 10, 2533-2555, https://doi.org/10.5194/amt-10-2533-2017, 2017.

Ding, J., Miyazaki, K., van der A, R. J., Mijling, B., Kurokawa, J.-I., Cho, S., Janssens-Maenhout, G., Zhang, Q., Liu, F., and Levelt, P. F.: Intercomparison of NOx emission inventories over East Asia, Atmos. Chem. Phys., 17, 10125-10141, https://doi.org/10.5194/acp-17-10125-2017, 2017.

Dragani, R., Benedetti, A., Flemming, J., Balsamo, G., Diamantakis, M., Geer, A.J., Hogan, R., Stockdale, T., Ades, M., Agusti-Panareda, A., Barré, J., Bechtold, P., Bozzo, A., Hersbach, H., Hólm, E., Kipling, Z., Inness, A., Letertre-Danczak, J., Massart, S., Matricardi, M., McNally, T., Parrington, M., Sandu, I., Soci, C., Vitart, F.: Atmospheric Composition priority developments for Numerical Weather Prediction. ECMWF Technical memorandum 833, doi:10.21957/5e0whui2y , 2018.

Errera, Q., Chabrillat, S., Christophe, Y., Debosscher, J., Hubert, D., Lahoz, W., Santee, M. L., Shiotani, M., Skachko, S., von Clarmann, T., and Walker, K.: Technical note: Reanalysis of Aura MLS Chemical Observations, Atmos. Chem. Phys. Discuss., https://doi.org/10.5194/acp-2019-530, in review, 2019.

Fleming, Z.L., Doherty, R.M., von Schneidemesser, E., Malley, C.S., Cooper, O.R., Pinto, J.P., Colette, A., Xu, X., Simpson, D., Schultz, M.G., Lefohn, A.S., Hamad, S., Moolla, R., Solberg, S. and Feng, Z.: Tropospheric Ozone Assessment Report: Present-day ozone distribution and trends relevant to human health. *Elem Sci Anth*, 6(1), p.12. DOI: http://doi.org/10.1525/elementa.273, 2018.

Flemming, J., Inness, A., Flentje, H., Huijnen, V., Moinat, P., Schultz, M. G., and Stein, O.: Coupling global chemistry transport models to ECMWF's integrated forecast system ECMWF technical memorandum 590, doi: 10.21957/z1hxhdhgo, 2009.

Flemming, J., Huijnen, V., Arteta, J., Bechtold, P., Beljaars, A., Blechschmidt, A.-M., Diamantakis, M., Engelen, R. J., Gaudel, A., Inness, A., Jones, L., Josse, B., Katragkou, E., Marecal, V., Peuch, V.-H., Richter, A., Schultz, M. G., Stein, O., and Tsikerdekis, A.: Tropospheric chemistry in the Integrated Forecasting System of ECMWF, Geosci. Model Dev., 8, 975-1003, https://doi.org/10.5194/gmd-8-975-2015, 2015.

Flemming, J., Benedetti, A., Inness, A., Engelen, R. J., Jones, L., Huijnen, V., Remy, S., Parrington, M., Suttie, M., Bozzo, A., Peuch, V.-H., Akritidis, D., and Katragkou, E.: The CAMS interim Reanalysis of Carbon Monoxide, Ozone and Aerosol for 2003–2015, Atmos. Chem. Phys., 17, 1945-1983, https://doi.org/10.5194/acp-17-1945-2017, 2017.

Flemming, J. and Inness, A.: Carbon Monoxide [in "State of the Climate in 2017"], B. Am. Meteorol. Soc., 99, S59–S61, 2018.

Fröhlich, C. and Lean, J., Solar radiative output and its variability: evidence and mechanisms. The Astron. Astrophys. Rev. 12: 273. https://doi.org/10.1007/s00159-004-0024-1, 2004.

995   Fu, D., Kulawik, S. S., Miyazaki, K., Bowman, K. W., Worden, J. R., Eldering, A., Livesey, N. J., Teixeira, J., Irion, F. W., Herman, R. L., Osterman, G. B., Liu, X., Levelt, P. F., Thompson, A. M., and Luo, M.: Retrievals of tropospheric ozone profiles from the synergism of AIRS and OMI: methodology and validation, Atmos. Meas. Tech., 11, 5587-5605, https://doi.org/10.5194/amt-11-5587-2018, 2018.

Gaudel, A., Cooper, O.R., Ancellet, G., Barret, B., Boynard, A., Burrows, J.P., Clerbaux, C., Coheur, P.-F., Cuesta, J.,
1000   Cuevas, E., Doniki, S., Dufour, G., Ebojie, F., Foret, G., Garcia, O., Granados Muños, M.J., Hannigan, J.W., Hase, F., Huang, G., Hassler, B., Hurtmans, D., Jaffe, D., Jones, N., Kalabokas, P., Kerridge, B., Kulawik, S.S., Latter, B., Leblanc, T., Le Flochmoën, E., Lin, W., Liu, J., Liu, X., Mahieu, E., McClure-Begley, A., Neu, J.L., Osman, M., Palm, M., Petetin, H., Petropavlovskikh, I., Querel, R., Rahpoe, N., Rozanov, A., Schultz, M.G., Schwab, J., Siddans, R., Smale, D., Steinbacher, M., Tanimoto, H., Tarasick, D.W., Thouret, V., Thompson, A.M., Trickl, T., Weatherhead, E.,
1005   Wespes, C., Worden, H.M., Vigouroux, C., Xu, X., Zeng, G. and Ziemke, J.: Tropospheric Ozone Assessment Report: Present-day distribution and trends of tropospheric ozone relevant to climate and global atmospheric chemistry model evaluation. Elem Sci Anth, 6(1), p.39. DOI: http://doi.org/10.1525/elementa.291, 2018.

Graedel, T. E., Bates, T. S., Bouwman, A. F., Cunnold, D., Dignon, J., Fung, I., Jacob, D. J., Lamb, B. K., Logan, J. A., Marland, G., Middleton, P., Pacyna, J. M., Placet, M., & Veldt, C., A compilation of inventories of emissions to the
1010   atmosphere, Global Biogeochem. Cy., 7, 1–26, 1993.

Hao, N., Koukouli, M. E., Inness, A., Valks, P., Loyola, D. G., Zimmer, W., Balis, D. S., Zyrichidou, I., Van Roozendael, M., Lerot, C., and Spurr, R. J. D.: GOME-2 total ozone columns from MetOp-A/MetOp-B and assimilation in the MACC system, Atmos. Meas. Tech., 7, 2937-2951, https://doi.org/10.5194/amt-7-2937-2014, 2014.

Hersbach, H., de Rosnay, P., Bell, B., Schepers, D., Simmons, A., Soci, C., Abdalla, S., Alonso-Balmaseda, M., Balsamo,
1015   G., Bechtold, P., Berrisford, P., Bidlot, J.-R., de Boisséson, E., Bonavita, M., Browne, P., Buizza, R., Dahlgren, P., Dee, D., Dragani, R., Diamantakis, M., Flemming, J., Forbes, R., Geer, A. J., Haiden, T., Hólm, E., Haimberger, L., Hogan, R., Horányi, A., Janiskova, M., Laloyaux, P., Lopez, P., Munoz-Sabater, J., Peubey, C., Radu, R., Richardson, D., Thépaut, J.-N., Vitart, F., Yang, X., Zsótér, E., and Zuo, H.: Operational global reanalysis: progress, future directions and synergies with NWP, ERA Report Series, Number 27, available at: https://www.ecmwf.int/node/18765 (last access: 15
1020   March 2019), 2018.

Hsu, J. and Prather, M. J.: Stratospheric variability and tropospheric ozone, J. Geophys. Res.-Atmos., 114, D06102, doi:10.1029/2008jd010942, 2009.

Huang, M., Carmichael, G. R., Pierce, R. B., Jo, D. S., Park, R. J., Flemming, J., Emmons, L. K., Bowman, K. W., Henze, D. K., Davila, Y., Sudo, K., Jonson, J. E., Tronstad Lund, M., Janssens-Maenhout, G., Dentener, F. J., Keating, T. J., Oetjen,
1025   H., and Payne, V. H.: Impact of intercontinental pollution transport on North American ozone air pollution: an HTAP phase 2 multi-model study, Atmos. Chem. Phys., 17, 5721–5750, https://doi.org/10.5194/acp-17-5721-2017, 2017.

Hunt, B. R., Kostelich, E. J., & Szunyogh, I., Efficient data assimilation for spatiotemporal chaos: a local ensemble transform Kalman filter, *Physica D*, 230, 112–126, 2007.

Huijnen, V., Flemming, J., Kaiser, J. W., Inness, A., Leitão, J., Heil, A., Eskes, H. J., Schultz, M. G., Benedetti, A., Hadji-
1030   Lazaro, J., Dufour, G., and Eremenko, M.: Hindcast experiments of tropospheric composition during the summer 2010 fires over western Russia, Atmos. Chem. Phys., 12, 4341-4364, https://doi.org/10.5194/acp-12-4341-2012, 2012.

Huijnen V., Wooster, M. J., Kaiser, J. W., Gaveau, D.L.A., Flemming, J., Parrington, M. Inness, A., Murdiyarso, D., Main, B. and van Weele, M.: Fire carbon emissions over maritime southeast Asia in 2015 largest since 1997, Scientific Reports, 6:26886, DOI: 10.1038/srep26886, 2016.

1035   Im, U., Christensen, J. H., Geels, C., Hansen, K. M., Brandt, J., Solazzo, E., Alyuz, U., Balzarini, A., Baro, R., Bellasio, R., Bianconi, R., Bieser, J., Colette, A., Curci, G., Farrow, A., Flemming, J., Fraser, A., Jimenez-Guerrero, P., Kitwiroon, N., Liu, P., Nopmongcol, U., Palacios-Peña, L., Pirovano, G., Pozzoli, L., Prank, M., Rose, R., Sokhi, R., Tuccella, P., Unal, A., Vivanco, M. G., Yarwood, G., Hogrefe, C., and Galmarini, S.: Influence of anthropogenic emissions and boundary conditions on multi-model simulations of major air pollutants over Europe and North America in the framework of
1040   AQMEII3, Atmos. Chem. Phys., 18, 8929-8952, https://doi.org/10.5194/acp-18-8929-2018, 2018.

Inness, A., Baier, F., Benedetti, A., Bouarar, I., Chabrillat, S., Clark, H., Clerbaux, C., Coheur, P., Engelen, R. J., Errera, Q., Flemming, J., George, M., Granier, C., Hadji-Lazaro, J., Huijnen, V., Hurtmans, D., Jones, L., Kaiser, J. W., Kapsomenakis, J., Lefever, K., Leitão, J., Razinger, M., Richter, A., Schultz, M. G., Simmons, A. J., Suttie, M., Stein, O., Thépaut, J.-N., Thouret, V., Vrekoussis, M., Zerefos, C., and the MACC team: The MACC reanalysis: an 8 yr data set of
1045   atmospheric composition, Atmos. Chem. Phys., 13, 4073-4109, https://doi.org/10.5194/acp-13-4073-2013, 2013.

Inness, A., Benedetti, A., Flemming, J., Huijnen, V., Kaiser, J. W., Parrington, M., and Remy, S.: The ENSO signal in atmospheric composition fields: emission-driven versus dynamically induced changes, Atmos. Chem. Phys., 15, 9083-9097, https://doi.org/10.5194/acp-15-9083-2015, 2015.

Inness, A., Ades, M., Agustí-Panareda, A., Barré, J., Benedictow, A., Blechschmidt, A.-M., Dominguez, J. J., Engelen, R.,
1050   Eskes, H., Flemming, J., Huijnen, V., Jones, L., Kipling, Z., Massart, S., Parrington, M., Peuch, V.-H., Razinger, M., Remy, S., Schulz, M., and Suttie, M.: The CAMS reanalysis of atmospheric composition, Atmos. Chem. Phys., 19, 3515-3556, https://doi.org/10.5194/acp-19-3515-2019, 2019.

Jiang, Z., B. C. McDonald, H. Worden, J. R. Worden, K. Miyazaki, Z. Qu, D. K. Henze, D. B. A. Jones, A. F. Arellano, E. V. Fischer, L. Zhu, and K. F. Boersma, Unexpected slowdown of US pollutant emission reduction in the last decade,
1055   Proceedings of the National Academy of Sciences, 201801191; DOI: 10.1073/pnas.1801191115, 2018.

Jonson, J. E., Schulz, M., Emmons, L., Flemming, J., Henze, D., Sudo, K., Tronstad Lund, M., Lin, M., Benedictow, A., Koffi, B., Dentener, F., Keating, T., Kivi, R., and Davila, Y.: The effects of intercontinental emission sources on European air pollution levels, Atmos. Chem. Phys., 18, 13655-13672, https://doi.org/10.5194/acp-18-13655-2018, 2018.

Kanaya, Y., Miyazaki, K., Taketani, F., Miyakawa, T., Takashima, H., Komazaki, Y., Pan, X., Kato, S., Sudo, K., Inoue, J.,
1060   Sato, K., and Oshima, K.: Ozone and carbon monoxide observations over open oceans on R/V Mirai from 67° S to 75° N during 2012 to 2017: Testing global chemical reanalysis in terms of Arctic processes, low ozone levels at low latitudes, and pollution transport, Atmos. Chem. Phys., https://doi.org/10.5194/acp-2018-1354, in press, 2019.

Katragkou, E., Zanis, P., Tsikerdekis, A., Kapsomenakis, J., Melas, D., Eskes, H., Flemming, J., Huijnen, V., Inness, A., Schultz, M. G., Stein, O., and Zerefos, C. S.: Evaluation of near-surface ozone over Europe from the MACC reanalysis,
1065   Geosci. Model Dev., 8, 2299-2314, https://doi.org/10.5194/gmd-8-2299-2015, 2015.

Knowland, K., Ott, L., Duncan, B., and Wargan, K.: Stratospheric Intrusion-Influenced Ozone Air Quality Exceedances Investigated in the NASA MERRA-2 Reanalysis, Geophys. Res. Lett., 44, 10691–10701, https://doi.org/10.1002/2017GL074532, 2017.

Lahoz, W. A. and Schneider, P.: Data assimilation: making sense of Earth Observation, *Front. Environ. Sci.*, 2, 16,
1070   doi:10.3389/fenvs.2014.00016, 2014.

Lerot, C., M. Van Roozendael, J. van Geffen, C. Fayt, R. Spurr, G. Lichtenberg, and A. von Bargen (2009), Six years of total ozone column measurements from SCIAMACHY nadir observations, Atmos. Meas. Tech., doi:10.5194/amt-2-87-2009.

Liang, C.-K., West, J. J., Silva, R. A., Bian, H., Chin, M., Davila, Y., Dentener, F. J., Emmons, L., Flemming, J., Folberth, G., Henze, D., Im, U., Jonson, J. E., Keating, T. J., Kucsera, T., Lenzen, A., Lin, M., Lund, M. T., Pan, X., Park, R. J.,

1075   Pierce, R. B., Sekiya, T., Sudo, K., and Takemura, T.: HTAP2 multi-model estimates of premature human mortality due to intercontinental transport of air pollution and emission sectors, Atmos. Chem. Phys., 18, 10497-10520, https://doi.org/10.5194/acp-18-10497-2018, 2018.

Liu, X., Bhartia, P. K., Chance, K., Froidevaux, L., Spurr, R. J. D., and Kurosu, T. P.: Validation of Ozone Monitoring Instrument (OMI) ozone profiles and stratospheric ozone columns with Microwave Limb Sounder (MLS) measurements,
1080   Atmos. Chem. Phys., 10, 2539-2549, https://doi.org/10.5194/acp-10-2539-2010, 2010.

Livesey, N. J., Read, W.G., Wagner, P. A., Froidevaux, L. , Lambert, A., Manney, G. L., Millán Valle, L. F., Pumphrey, H. C., Santee, M. L., Schwartz, M. J., Wang, S., Fuller, R. A., Jarnot, R. F., Knosp, B. W., Martinez, E., Lay, R. R.: Aura Microwave Limb Sounder (MLS) Version 4.2x Level2 data quality and description document, Tech. Rep. JPL D33509
1085   Rev. D, Jet Propul. Lab., Pasadena, CA, 2018.

McPeters, R. D., P. K. Bhartia, D. Haffner, G. J. Labow, and L. Flynn: The version 8.6 SBUV ozone data record: An
1090   overview, J. Geophys. Res. Atmos., 118, 8032–8039, doi:10.1002/jgrd.50597, 2013.

Ménard, R. and Chang, L.: Assimilation of Stratospheric Chemical Tracer Observations Using a Kalman Filter. Part II: χ^2-Validated Results and Analysis of Variance and Correlation Dynamics. Mon. Wea. Rev.,1282672–2686, https://doi.org/10.1175/1520-0493(2000)128<2672:AOSCTO>2.0.CO;2

Miyazaki, K., Eskes, H. J., & Sudo, K., Global NOx emission estimates derived from an assimilation of OMI tropospheric
1095   NO$_2$ columns, *Atmospheric Chemistry and Physics*, 12, 2263-2288, doi:10.5194/acp-12-2263-2012, 2012a.

Miyazaki, K., Eskes, H. J., Sudo, K., Takigawa, M., van Weele, M., & Boersma, K. F., Simultaneous assimilation of satellite NO$_2$, O$_3$, CO, and HNO$_3$ data for the analysis of tropospheric chemical composition and emissions, *Atmospheric Chemistry and Physics*, 12, 9545-9579, doi:10.5194/acp-12-9545-2012, 2012b.

Miyazaki, K., H. Eskes, K. Sudo, & C. Zhang, Global lightning NOx production estimated by an assimilation of multiple
1100   satellite datasets, *Atmospheric Chemistry and Physics*, 14, 3277-3305, 2014.

Miyazaki, K., Eskes, H. J., & Sudo, K., A tropospheric chemistry reanalysis for the years 2005–2012 based on an assimilation of OMI, MLS, TES, and MOPITT satellite data, *Atmos. Chem. Phys.*, 15, 8315-8348, doi:10.5194/acp-15-8315-2015, 2015.

Miyazaki, K. & Bowman, K., Evaluation of ACCMIP ozone simulations and ozonesonde sampling biases using a satellite-
1105   based multi-constituent chemical reanalysis, *Atmos. Chem. Phys.*, 17, 8285-8312, https://doi.org/10.5194/acp-17-8285-2017, 2017a.

Miyazaki, K., Eskes, H., Sudo, K., Boersma, K. F., Bowman, K., & Kanaya, Y. (2017), Decadal changes in global surface NOx emissions from multi-constituent satellite data assimilation, *Atmos. Chem. Phys.*, 17, 807-837, doi:10.5194/acp-17-807-2017b.

1110 Miyazaki. K., T. Sekiya, D. Fu, K. W. Bowman, S. S. Kulawik, K. Sudo, T. Walker, Y. Kanaya, M. Takigawa, K. Ogochi, H. Eskes, K. F. Boersma, A. M. Thompson, B. Gaubert, J. Barre, L. K. Emmons: Balance of emission and dynamical controls on ozone during KORUS-AQ from multi-constituent satellite data assimilation, *Journal of Geophysical Research: Atmospheres*, 124, 387–413. https://doi.org/10.1029/2018JD028912, 2019a.

Miyazaki, K., Bowman, K. W., Yumimoto, K., Walker, T., and Sudo, K.: Evaluation of a multi-model, multi-constituent
1115   assimilation framework for tropospheric chemical reanalysis, Atmos. Chem. Phys. Discuss., https://doi.org/10.5194/acp-2019-645, in review, 2019.

Monks, P. S., Archibald, A. T., Colette, A., Cooper, O., Coyle, M., Derwent, R., Fowler, D., Granier, C., Law, K. S., Mills, G. E., Stevenson, D. S., Tarasova, O., Thouret, V., von Schneidemesser, E., Sommariva, R., Wild, O., and Williams, M. L.: Tropospheric ozone and its precursors from the urban to the global scale from air quality to short-lived climate forcer, Atmos. Chem. Phys., 15, 8889–8973, https://doi.org/10.5194/acp-15-8889-2015, 2015.

Morgenstern, O., Stone, K. A., Schofield, R., Akiyoshi, H., Yamashita, Y., Kinnison, D. E., Garcia, R. R., Sudo, K., Plummer, D. A., Scinocca, J., Oman, L. D., Manyin, M. E., Zeng, G., Rozanov, E., Stenke, A., Revell, L. E., Pitari, G., Mancini, E., Di Genova, G., Visioni, D., Dhomse, S. S., and Chipperfield, M. P.: Ozone sensitivity to varying greenhouse gases and ozone-depleting substances in CCMI-1 simulations, Atmos. Chem. Phys., 18, 1091-1114, https://doi.org/10.5194/acp-18-1091-2018, 2018.

Munro, R., R. Siddans, W. J. Reburn, and B. J. Kerridge, Direct measurements of tropospheric ozone distributions from space, Nature, 392, 168–171, 1998.

Nédélec, P, Blot, R, Boulanger, D, Athier, G, Cousin, J, Gautron, B, Petzold, A, Volz-Thomas, A and Thouret, V. 2015. Instrumentation on commercial aircraft for monitoring the atmospheric composition on a global scale: the IAGOS system, technical overview of ozone and carbon monoxide measurements. Tellus B 67. DOI: 10.3402/tellusb.v67.27791

Neu, J. L., Flury, T., Manney, G. L., Santee, M. L., Livesey, N. J., Worden, J.: Tropospheric ozone variations governed by changes in stratospheric circulation. Nature Geoscience 7, pp 340–344 (2014). Doi: 10.1038/ngeo2138

Ordóñez, C., Elguindi, N., Stein, O., Huijnen, V., Flemming, J., Inness, A., Flentje, H., Katragkou, E., Moinat, P., Peuch, V.-H., Segers, A., Thouret, V., Athier, G., van Weele, M., Zerefos, C. S., Cammas, J.-P., and Schultz, M. G.: Global model simulations of air pollution during the 2003 European heat wave, Atmos. Chem. Phys., 10, 789-815, https://doi.org/10.5194/acp-10-789-2010, 2010.

Parrish, DD, Lamarque, J-F, Naik, V, Horowitz, L, Shindell, DT, et al.. Long-term changes in lower tropospheric baseline ozone concentrations: Comparing chemistry-climate models and observations at northern mid-latitudes. J. Geophys. Res . 119(9): 5719–5736. DOI: 10.1002/2013JD021435, 2014.

Schultz M. G., Schröder, S., Lyapina, O., Cooper, O., Galbally, I., Petropavlovskikh, I., et al.: Tropospheric Ozone Assessment Report: Database and Metrics Data of Global Surface Ozone Observations, Elem. Sci. Anth., 5, 58, https://doi.org/10.1525/elementa.244, 2017.

Schultz, M. G., Schröder, S., Lyapina, O., Cooper, O. R., Galbally, I., Petropavlovskikh, I., Schneidemesser, E. V., Tanimoto, H., Elshorbany, Y., Naja, M., Seguel, R. J., Dauert, U., Eckhardt, P., Feigenspan, S., Fiebig, M., Hjellbrekke, A.-G., Hong, Y.-D., Kjeld, P. C., Koide, H., Lear, G., Tarasick, D., Ueno, M., Wallasch, M., Baumgardner, D., Chuang, M.-T., Gillett, R., Lee, M., Molloy, S., Moolla, R., Wang, T., Sharps, K., Adame, J. A., Ancellet, G., Apadula, F., Artaxo, P., Barlasina, M. E., Bogucka, M., Bonasoni, P., Chang, L., Colomb, A., Cuevas-Agulló, E., Cupeiro, M., Degorska, A., Ding, A., Fröhlich, M., Frolova, M., Gadhavi, H., Gheusi, F., Gilge, S., Gonzalez, M. Y., Gros, V., Hamad, S. H., Helmig, D., Henriques, D., Hermansen, O., Holla, R., Hueber, J., Im, U., Jaffe, D. A., Komala, N., Kubistin, D., Lam, K.-S., Laurila, T., Lee, H., Levy, I., Mazzoleni, C., Mazzoleni, L. R., McClure-Begley, A., Mohamad, M., Murovec, M., Navarro-Comas, M., Nicodim, F., Parrish, D., Read, K. A., Reid, N., Ries, L., Saxena, P., Schwab, J. J., Scorgie, Y., Senik, I., Simmonds, P., Sinha, V., Skorokhod, A. I., Spain, G., Spangl, W., Spoor, R., Springston, S. R., Steer, K., Steinbacher, M., Suharguniyawan, E., Torre, P., Trickl, T., Weili, L., Weller, R., Xiaobin, X., Xue, L., and Zhiqiang, M.: Tropospheric Ozone Assessment Report, links to Global surface ozone datasets, PANGAEA, https://doi.org/10.1594/PANGAEA.876108, 2017.

Schwartz, M., Froidevaux, L., Livesey, N. and Read, W. (2015), MLS/Aura Level 2 Ozone (O3) Mixing Ratio V004, Greenbelt, 25 MD, USA, Goddard Earth Sciences Data and Information Services Center (GES DISC), Accessed: [20180718], 10.5067/Aura/MLS/DATA2017, 2015.

Sekiya, T., Miyazaki, K., Ogochi, K., Sudo, K., and Takigawa, M.: Global high-resolution simulations of tropospheric nitrogen dioxide using CHASER V4.0, Geosci. Model Dev., 11, 959-988, https://doi.org/10.5194/gmd-11-959-2018, 2018.

Sudo, K., Takahashi, M., and Akimoto, H.: CHASER: a global chemical model of the troposphere 2. Model results and evaluation, J. Geophys. Res., 107, 4586, doi:10.1029/2001JD001114, 2002.

Struzewska, J. and Kaminski, J. W.: Formation and transport of photooxidants over Europe during the July 2006 heat wave – observations and GEM-AQ model simulations, Atmos. Chem. Phys., 8, 721-736, https://doi.org/10.5194/acp-8-721-2008, 2008.

Tang, W., Arellano, A. F., Gaubert, B., Miyazaki, K., and Worden, H. M.: Satellite data reveal a common combustion emission pathway for major cities in China, Atmos. Chem. Phys., 19, 4269-4288, https://doi.org/10.5194/acp-19-4269-2019, 2019.

Thompson, A.M, R. M. Stauffer, T. P. Boyle, D. E. Kollonige, K. Miyazaki, M. Tzortziou, J. R. Herman, C. N. Jordan, B. T. Lamb, B. N. Duncan, Comparison of Near-surface NO_2 Pollution with Pandora Total Column NO_2 during the Korea-United States Ocean Color (KORUS OC) Campaign, , J. Geophys. Res., in review, 2019.

Thouret, V., Cammas, J.-P., Sauvage, B., Athier, G., Zbinden, R., Nédélec, P., Simon, P., and Karcher, F.: Tropopause referenced ozone climatology and inter-annual variability (1994–2003) from the MOZAIC programme, Atmos. Chem. Phys., 6, 1033-1051, https://doi.org/10.5194/acp-6-1033-2006, 2006.

Tilmes, S., Lamarque, J.-F., Emmons, L. K., Conley, A., Schultz, M. G., Saunois, M., Thouret, V., Thompson, A. M., Oltmans, S. J., Johnson, B., and Tarasick, D.: Technical Note: Ozonesonde climatology between 1995 and 2011: description, evaluation and applications, Atmos. Chem. Phys., 12, 7475–7497, https://doi.org/10.5194/acp-12-7475-2012, 2012.

Travis, K. R., Jacob, D. J., Fisher, J. A., Kim, P. S., Marais, E. A., Zhu, L., Yu, K., Miller, C. C., Yantosca, R. M., Sulprizio, M. P., Thompson, A. M., Wennberg, P. O., Crounse, J. D., St. Clair, J. M., Cohen, R. C., Laughner, J. L., Dibb, J. E., Hall, S. R., Ullmann, K., Wolfe, G. M., Pollack, I. B., Peischl, J., Neuman, J. A., and Zhou, X.: Why do models overestimate surface ozone in the Southeast United States?, Atmos. Chem. Phys., 16, 13561-13577, https://doi.org/10.5194/acp-16-13561-2016, 2016.

van der A, R. J., Mijling, B., Ding, J., Koukouli, M. E., Liu, F., Li, Q., Mao, H., and Theys, N.: Cleaning up the air: effectiveness of air quality policy for SO2 and NOx emissions in China, Atmos. Chem. Phys., 17, 1775–1789, https://doi.org/10.5194/acp-17-1775-2017, 2017.

Van Dingenen, R, Dentener, FJ, Raes, F, Krol, MC, Emberson, L & Cofala, J: 'The global impact of ozone on agricultural crop yields under current and future air quality legislation', Atmospheric Environment, vol. 43, no. 3, pp. 604-618. https://doi.org/10.1016/j.atmosenv.2008.10.033, 2009.

Verstraeten, W. W., Neu, J. L., Williams, J. E., Bowman, K. W., Worden, J. R., and Boersma, K. F.: Rapid increases in tropospheric ozone production and export from China, Nat. Geosci., 8, 690–695, doi:10.1038/ngeo2493, 2015.

von Clarmann, T., et al., Retrieval of temperature and tangent altitude pointing from limb emission spectra recorded from space by the Michelson Interferometer for Passive Atmospheric Sounding (MIPAS), J. Geophys. Res., 108(D23), 4736, doi:10.1029/2003JD003602, 2003.

von Clarmann, T., Höpfner, M., Kellmann, S., Linden, A., Chauhan, S., Funke, B., Grabowski, U., Glatthor, N., Kiefer, M., Schieferdecker, T., Stiller, G. P., and Versick, S.: Retrieval of temperature, H2O, O3, HNO3, CH4, N2O, ClONO2 and ClO from MIPAS reduced resolution nominal mode limb emission measurements, Atmos. Meas. Tech., 2, 159–175, doi:10.5194/amt-2-159- 2009, 2009.Watanabe, S., Hajima, T., Sudo, K., Nagashima, T., Takemura, T., Okajima, H., Nozawa, T., Kawase, H., Abe, M., Yokohata, T., Ise, T., Sato, H., Kato, E., Takata, K., Emori, S., & Kawamiya, M.,

MIROC-ESM 2010: model description and basic results of CMIP5-20c3m experiments, *Geosci. Model Dev.*, 4, 845–872, https://doi.org/10.5194/gmd-4-845-2011, 2011.

Williams, R. S., Hegglin, M. I., Kerridge, B. J., Jöckel, P., Latter, B. G., and Plummer, D. A.: Characterising the seasonal and geographical variability in tropospheric ozone, stratospheric influence and recent changes, Atmos. Chem. Phys., 19, 3589-3620, https://doi.org/10.5194/acp-19-3589-2019, 2019.

Wolter, K., and M. S. Timlin: Measuring the strength of ENSO events - how does 1997/98 rank? Weather, 53, 315-324, 1998.

Young, P. J., Archibald, A. T., Bowman, K. W., Lamarque, J.-F., Naik, V., Stevenson, D. S., Tilmes, S., Voulgarakis, A., Wild, O., Bergmann, D., Cameron-Smith, P., Cionni, I., Collins, W. J., Dalsøren, S. B., Doherty, R. M., Eyring, V., Faluvegi, G., Horowitz, L. W., Josse, B., Lee, Y. H., MacKenzie, I. A., Nagashima, T., Plummer, D. A., Righi, M., Rumbold, S. T., Skeie, R. B., Shindell, D. T., Strode, S. A., Sudo, K., Szopa, S., and Zeng, G.: Pre-industrial to end 21st century projections of tropospheric ozone from the Atmospheric Chemistry and Climate Model Intercomparison Project (ACCMIP), Atmos. Chem. Phys., 13, 2063-2090, https://doi.org/10.5194/acp-13-2063-2013, 2013.

Ziemke, J. R., and S. Chandra (2003), La Nina and El Nino—induced variabilities of ozone in the tropical lower atmosphere during 1970–2001, Geophys. Res. Lett., 30, 1142, doi: 10.1029/2002GL016387, 3.

Ziemke, J. R., Oman, L. D., Strode, S. A., Douglass, A. R., Olsen, M. A., McPeters, R. D., Bhartia, P. K., Froidevaux, L., Labow, G. J., Witte, J. C., Thompson, A. M., Haffner, D. P., Kramarova, N. A., Frith, S. M., Huang, L.-K., Jaross, G. R., Seftor, C. J., Deland, M. T., and Taylor, S. L.: Trends in global tropospheric ozone inferred from a composite record of TOMS/OMI/MLS/OMPS satellite measurements and the MERRA-2 GMI simulation , Atmos. Chem. Phys., 19, 3257-3269, https://doi.org/10.5194/acp-19-3257-2019, 2019.